



2  
1 2

This is to certify that the  
thesis entitled

HYDRODYNAMICS AND LONGITUDINAL DISPERSION  
IN THE RED CEDAR RIVER

presented by

IRFAN ASLAM

has been accepted towards fulfillment  
of the requirements for the

Master of  
Science

degree in

Environmental Engineering

*Thomas A. Urie*

Major Professor's Signature

*December 13, 2002*

Date

**LIBRARY**  
**Michigan State**  
**University**

**PLACE IN RETURN BOX** to remove this checkout from your record.

**TO AVOID FINES** return on or before date due.

**MAY BE RECALLED** with earlier due date if requested.

DATE DUE	DATE DUE	DATE DUE
MAR 30 2004		
JAN 10 2005 JAN 07 04		
JUL 16 2005		
07 23 05		
FEB 28 2006		
JUN 08 2006 MAY 01 2006 04 24 06		
OCT 12 2009		

**HYDRODYNAMICS AND LONGITUDINAL DISPERSION IN THE RED CEDAR  
RIVER**

**By**

**Irfan Aslam**

**A THESIS**

**Submitted to  
Michigan State University  
in partial fulfilment of the requirements  
for the degree of**

**MASTER OF SCIENCE**

**Department of Civil and Environmental Engineering**

**2002**

## **ABSTRACT**

### **HYDRODYNAMICS AND LONGITUDINAL DISPERSION IN RED CEDAR RIVER**

**By**

**Irfan Aslam**

A one-dimensional hydrodynamic model for the Red Cedar River based on the EPA version of DYNHYD5 is presented herein for simulating the unsteady flow conditions. The model framework was built using bathymetric data from flood insurance studies. Channel geometry of the model network was kept sufficiently simple so as to yield characteristic results in a single spatial dimension. The objective was to accurately predict the hydrodynamic parameters for use in simulating contaminant transport through the river reach. A series of dye dispersion studies conducted for different flow conditions offer a characterization of the river reach with regards to longitudinal dispersion, which is an essential component in contaminant transport. The results of dye dispersion studies confirm the variability of dispersion with space and time. The model itself and the empirical equation developed for predicting the dispersion coefficient at any point within the reach bounds can be used as a base for simulating contaminant transport by the water quality model.

## ACKNOWLEDGMENTS

I would like to express my special thanks to Dr. Thomas C. Voice for his advice and guidance during this study. I also feel obliged to express my gratitude to Dr. M.S Phanikumar and Dr. David T. Long who consistently guided me to achieve my objective with valuable suggestions. I also acknowledge the cooperation by volunteer students who worked in the field to collect data during the dye studies.

## TABLE OF CONTENTS

ACKNOWLEDGMENTS .....	iii
1. INTRODUCTION .....	1
<b>1.2 Scope Of Study .....</b>	<b>4</b>
2. DESCRIPTION OF THE STUDY AREA .....	5
<b>2.1 Physical Settings.....</b>	<b>5</b>
<b>2.2 Flow Variations in Red Cedar .....</b>	<b>8</b>
3. LITERATURE REVIEW .....	10
4. METHODOLOGY .....	19
<b>4.1 Selection of Model.....</b>	<b>19</b>
<b>4.2 Fluorescein As A Water Tracer.....</b>	<b>20</b>
<b>4.3 Model Implementation .....</b>	<b>21</b>
<b>4.4 Model Segmentation .....</b>	<b>22</b>
<b>4.5 Tracer Tests.....</b>	<b>23</b>
<b>4.6 Data Collection.....</b>	<b>24</b>
<b>4.7 Manning's Roughness Coefficient.....</b>	<b>25</b>
5. RESULTS AND DISCUSSION .....	27
<b>5.1 Model Calibration.....</b>	<b>27</b>
<b>5.2 Hydrodynamics .....</b>	<b>29</b>
<b>5.3 Effect of Grid On Model Performance .....</b>	<b>33</b>
<b>5.4 Effect of Time Step on Model Performance .....</b>	<b>38</b>
<b>5.5 Time of Travel.....</b>	<b>41</b>
<b>5.6 Dispersion by Moments Method.....</b>	<b>49</b>
<b>5.7 Dispersion By Mass Transport.....</b>	<b>52</b>
6. CONCLUSIONS.....	69

7. APPENDICES .....	71
<b>Appendix A</b> <b>Junction and Channel Properties .....</b>	<b>71</b>
<b>Appendix B</b> <b>Input File.....</b>	<b>75</b>
<b>Appendix C</b> <b>Field Data.....</b>	<b>82</b>
<b>Appendix D</b> <b>Time-Concentration Data-Dye Release 1.....</b>	<b>84</b>
<b>Appendix E</b> <b>Time-Concentration Data-Dye Release 2.....</b>	<b>86</b>
<b>Appendix F</b> <b>Time-Concentration Data-Dye Release 3.....</b>	<b>88</b>
<b>Appendix G</b> <b>Time-Concentration Data-Dye Release 4.....</b>	<b>90</b>
<b>Appendix H</b> <b>Time-Concentration Data-Dye Release 5.....</b>	<b>92</b>
8. BIBLIOGRAPHY .....	94



**TABLE****Page**

Table 5-1	Manning's Roughness Coefficients.....	28
Table 5-2.	Regression statistics for hydrodynamic variables. ....	33
Table 5-3.	Time of travel data-dye release 1 (May 17, 2002). ....	42
Table 5-4.	Time of travel data-dye release 2 (May 31, 2002). ....	43
Table 5-5.	Time of travel data-dye release 3 (Jun 6, 2002). ....	44
Table 5-6.	Time of travel data-dye release 4 (Jun 21, 2002). ....	45
Table 5-7.	Time of travel data-dye release 5 (Jun 25, 2002). ....	46
Table 5-8	Dispersion Coefficients By Moments Method .....	51
Table 5-9	Dispersion coefficients calculated using the mass transport equation.....	53
Table 5-10.	Variation in concentration across a transect indicating the state of lateral mixing. ....	56
Table 5-11.	Area under time-concentration curves for calculated concentration. ....	58
Table 5-12.	Area under time-concentration curves for observed concentrations.....	59
Table 5-13.	Comparison of areas under the time-concentration curve for predicted and observed concentrations.....	59
Table 5-14.	Comparison of calculated and predicted dispersion coefficients.....	64

## FIGURE

	Page
Figure 2-1. Map showing Red Cedar River Basin from Cedar Lake to the confluence point of Grand River and Cedar River (Davood 1960).....	6
Figure 2-2. River profile in the study reach.....	7
Figure 2-3. Mean annual stream flow in Red Cedar River from yr 1932-2000 .....	8
Figure 2-4. Mean monthly stream flow in Red Cedar River for yr 2001 .....	9
Figure 5-1. Predicted and measured velocity at Library Bridge (4-11 April, 02). ....	29
Figure 5-2. Predicted and measured head at Library Bridge (4-11 April, 02).....	30
Figure 5-3. Predicted and measured flow at Library Bridge (4-11 April, 02).....	30
Figure 5-4. Predicted and measured velocity at Kellogg Bridge (4-11 April, 02). ...	31
Figure 5-5. Predicted and measured head at Kellogg Bridge (4-11 April, 02).....	31
Figure 5-6. Predicted and measured flow at Kellogg Bridge (4-11 April, 02).....	32
Figure 5-7. Effect of different grids on predicted velocity at the Library Bridge. ....	35
Figure 5-8. Effect of different grids on predicted head at the Library Bridge.....	35
Figure 5-9. Effect of grid on predicted flow at the Library Bridge. ....	36
Figure 5-10. Effect of different grids on predicted velocity at the Kellogg Bridge. ...	36
Figure 5-11. Effect of different grids on predicted head at the Kellogg Bridge.....	37
Figure 5-12. Effect of different grids on predicted flow at the Kellogg Bridge.....	37
Figure 5-13. Effect of different time step size on predicted velocity at Library Bridge.....	39
Figure 5-14. Effect of different time step size on predicted head at Library Bridge...	39
Figure 5-15. Effect of different time step size on predicted velocity at Kellogg Bridge.....	40
Figure 5-16. Effect of different time step size on predicted head at Kellogg Bridge..	40
Figure 5-17. Time-concentration curves-dye release 1 (May 17, 2002). ....	42

Figure 5-18.	Time-concentration curves-dye release 2 (May 31, 2002). .....	43
Figure 5-19.	Time-concentration curves-dye release 3 (Jun 6, 2002). .....	44
Figure 5-20.	Time-concentration curve-dye release 4 (Jun 21, 2002).....	45
Figure 5-21.	Time-concentration curves-dye release 5 (Jun 25, 2002). .....	46
Figure 5-22.	Time of arrival of leading edge, peak and trailing edge of the dye cloud at Farm Lane Bridge for different flow conditions.....	48
Figure 5-23.	Time of arrival of leading edge, peak and trailing edge of the dye cloud at Kellogg Bridge for different flow conditions. ....	48
Figure 5-24.	Time of arrival of leading edge, peak and trailing edge of the dye cloud at Kalamazoo Bridge for different flow conditions. ....	49
Figure 5-25.	Dispersion coefficients calculated using moments method for medium flow conditions.....	51
Figure 5-26.	Dispersion coefficient calculated using mass transport equation under different flow conditions.....	54
Figure 5-27.	Dispersion coefficient at different downstream sampling locations.....	55
Figure 5-28.	Predicted and observed concentration at 16.82 m <sup>3</sup> /sec flow.....	61
Figure 5-29.	Predicted and observed concentration at 14.41 m <sup>3</sup> /sec flow.....	61
Figure 5-30.	Predicted and observed concentration at 19.3 m <sup>3</sup> /sec flow.....	62
Figure 5-31.	Predicted and observed concentration at 2.49 m <sup>3</sup> /sec flow.....	62
Figure 5-32.	Predicted and observed concentration at 2.06 m <sup>3</sup> /sec flow.....	63
Figure 5-33.	Relation between calculated and predicted dispersion coefficients.....	64
Figure 5-34.	Calculated and observed peak arrival time. ....	65
Figure 5-35.	Predicted and observed concentration using empirical relations at 16.82 m <sup>3</sup> /sec flow.....	67
Figure 5-36.	Predicted and observed concentration using empirical relations at 14.41 m <sup>3</sup> /sec flow.....	67

Figure 5-37	Predicted and observed concentration using empirical relations at 19.06	
	m <sup>3</sup> /sec flow.....	68

# 1. INTRODUCTION

## 1.1 Overview

There are two basic reasons for representing natural water systems through mathematical modelling. The first is to increase the level of understanding of the cause-effect relationship operative in the evaluation of water quality. The second is to apply that increased understanding to aid in decision-making processes (Thomann 1982). In surface water quality modelling, characterizing the hydrodynamics correctly and quantifying dispersion accurately is essential to develop numerical tools that are sufficiently robust in their predictive capacity. Inclusion of longitudinal dispersion enhances realism and accuracy in the assessment of transport in streams by accounting for contaminant mixing and it is essential when longitudinal concentration gradients exist (Koussis and Mirasol 1998).

Hydrodynamic models are deterministic in nature but range considerably in complexity and level of mathematical sophistication. A hydrodynamic model can be a simple one-dimensional model with vertical and lateral averaging and on the other hand, can also be a very complex three-dimensional model taking into account the lateral and vertical stratification of the parameters. The majority of these models, whether one, two or three-dimensional, rely on the numerical solution of the basic hydrodynamic equations of flow, commonly known as St. Venant wave propagation equations (Ambrose 1993). Research of flow simulation modelling in riverine systems began in 1950's primarily by scientists in the U.S Geological Survey (Schaffranek and Goldberg 1981). The objective

was to provide a strong physical basis for the development of methods which could determine unsteady flows in channels affected by tides, flood waves or hydropower regulation where flow inertial effects were appreciable. Various numerical methods for treating the St. Venent wave-propagation equations were studied and various models were constructed and reported in the literature. The earliest models were designed to treat only a single reach since the numerical methods were primitive and computational capabilities were limited (Schaffranek and Goldberg 1981). In the early 1970's the use of branch-channel network schemes started which gave rise to a new field for the development of computationally efficient models. Important aspects of these models are the channel properties, cross-sectional geometry, initial and boundary conditions and the grid to adequately capture the desired hydrodynamic properties. Nevertheless, the predictive ability of numerical and hydraulic models cannot be fully established and no model can reproduce all that is related to external reality (Fischer 1981). One of the major issues has been the accurate prediction of the longitudinal dispersion, which is considered as one of the major process contributing towards concentration gradients.

Dispersion is the scattering of the particles in water that controls the concentration of a constituent as it is transported downstream. This scattering takes place vertically, transversely and longitudinally. Spreading in the direction of flow is primarily caused by velocity profile in the cross-section and is referred to as "shear flow" (Fischer 1979). Mixing in the vertical direction takes place first followed by mixing in transverse direction. Once the cross-sectional mixing is complete, the process of longitudinal dispersion is the most important mechanism, erasing all longitudinal concentration gradients (Fischer et al. 1979). Therefore in order to apply any model for the prediction

of concentrations at a distance downstream from the point of discharge, selection of a proper dispersion coefficient is most important and also the most difficult task (Seo and Cheong 1998).

The Red Cedar River meanders through the campus of Michigan State University over a stretch of approximately 5 km and is unique with regards to the layout as a number of outfalls draining the campus area feed it with pollutants. The nature of the pollutants varies depending on the sub-areas being drained by the outfalls. The resulting run-off may be from parking lots, walkways, lawns or agricultural farms, which enter the stream at different locations throughout. The reach also offers a unique study potential in terms of a number of bridges over the river, which makes the sampling possible on these locations at any point across the river width and offer an opportunity to study the variations in the hydrodynamics and contaminant transport over short distances.

The use of fluorescent dyes and tracing techniques provide a means for measuring the time of travel and dispersion characteristics of steady and gradually varied flow in streams. Measurements of the dispersion and concentration of dyes give insight into the behaviour of soluble contaminants that may be introduced into a stream. The concentration of dye in the sample is directly proportional to its fluorescence. A plot of concentration against time defines the passage of the dye cloud at each sampling site. Time of travel is measured by observing the time required for movement of the dye cloud between sampling sites.

## 1.2 Scope Of Study

Purpose of this study was to build a foundation for a one-dimensional water quality model for the Red Cedar River, which has its base principally in correctly establishing the hydrodynamics and dispersion. Keeping this specific purpose in mind, the study objectives aimed at:

- a. Developing a hydrodynamic model of Red Cedar River, which could predict the hydrodynamics with a reasonable accuracy.
- b. Quantifying the longitudinal dispersion under varying conditions of flow.



## 2. DESCRIPTION OF THE STUDY AREA

### 2.1 Physical Settings

The Red Cedar River is a warm water stream in south central Michigan. It originates as an outflow from Cedar Lake, located in Marion Township, Livingston County, Michigan. The stream flows past the communities of Fowlerville, Webberville, Williamston and Okemos before entering the East Lansing and Michigan State University area (Figure 2-1). Then it connects with the Grand River in Lansing (Ingham County, Michigan). Total stream length is 71.13 km. The river and its tributaries drain an area of about 1230.25 km<sup>2</sup>, one fourth of which is drained by Sycamore Creek. The river has an average gradient of 0.475 m/km, with about one-half of the fall occurring within the uppermost one-third of the river (Davood 1960). The bottom elevations were obtained from flood insurance studies done for Cedar River by Snell Environmental Group (Nalluswami 1978). The profile of the study section shows an average slope of 0.413 meter per kilometre for the river reach through MSU campus (Figure 2-2). The elevation of Cedar Lake is 284.68 m above sea level and the confluence of Cedar River with Grand River is at an elevation of 249.02 m above sea level. A USGS gauging station is located at the southwest abutment of the Farm Lane Bridge with the exact location being 42°43'40" latitude and 84°28'40" longitude. The gage datum is 251.27 meters above sea level and it measures the runoff from about 919.45 (74.73 %) km<sup>2</sup> of the basin. The mean annual temperature for the area is 8.2 °C, with a winter mean of approximately -4.4 °C



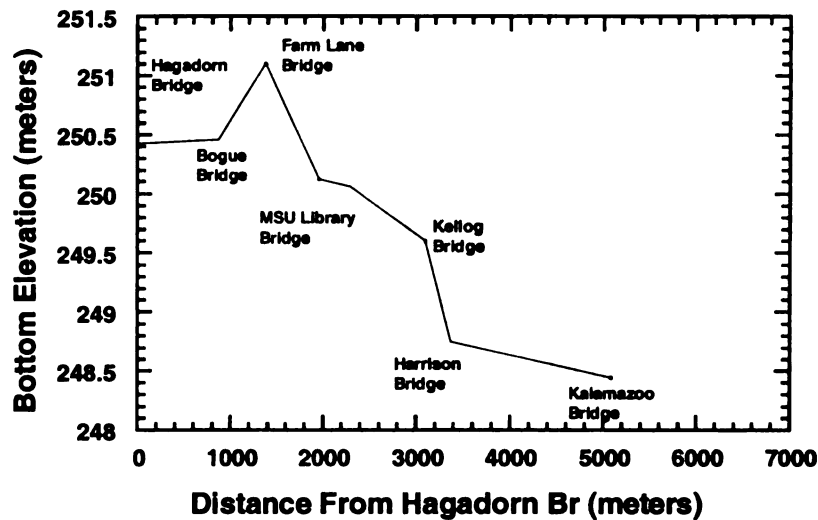


Figure 2-2 River profile in the study reach

The study section within the Michigan State University starts from Hagadorn Road Bridge at the upstream boundary and ends at Kalamazoo Street Bridge. The study section is 5.079 km long and varies from approximately 16 meters to 40 meters in width with an average width of 28 meters. Throughout the entire reach, 67 outfalls of varying sizes drain into the river. Fifty-nine out of sixty seven outfalls exist on the university maps prepared by the MSU Physical Plant. A weir is located opposite to the MSU main library. The backwaters of this weir extend upstream a short distance and cause an impoundment of water resulting in low velocity in the section. Downstream of the weir is a steep slope, which causes the water to gain energy due to an increase in head. This also causes re-aeration of water thereby improving the dissolved oxygen levels. Above the weir, the bottom is principally muddy mixed with rock debris; however, the banks are extensively

vegetated at places. Below the weir the bottom is coarse gravel and sand covered by a thin covering of silt and detritus. The banks are forested in some areas but much of the river study section runs along parking lots and lawns of Michigan State University.

## 2.2 Flow Variations in Red Cedar

Statistical analysis of the annual stream flow (Figure 2-3) shows a variation in the flow in various years with a mean of 214.6 ft<sup>3</sup>/sec and a standard deviation of 79.17 ft<sup>3</sup>/sec, which is 36.9% of the mean annual stream flow. A plot of the mean monthly flows for the year 2001 shows the seasonal variation in the stream flow (Figure 2-4). Diurnal variations in the flow were also observed from time to time, which confirm the need for a model that can handle transient flow.

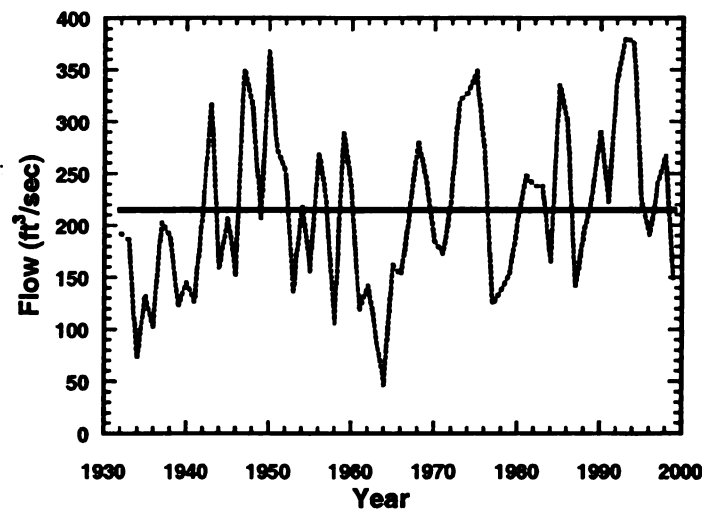


Figure 2-3. Mean annual stream flow in Red Cedar River from yr 1932-2000.  
(Source:[http://waterdata.sugs.gov/mi/nwis/annual/?site\\_no=04112500&agency\\_cd=USGS](http://waterdata.sugs.gov/mi/nwis/annual/?site_no=04112500&agency_cd=USGS))

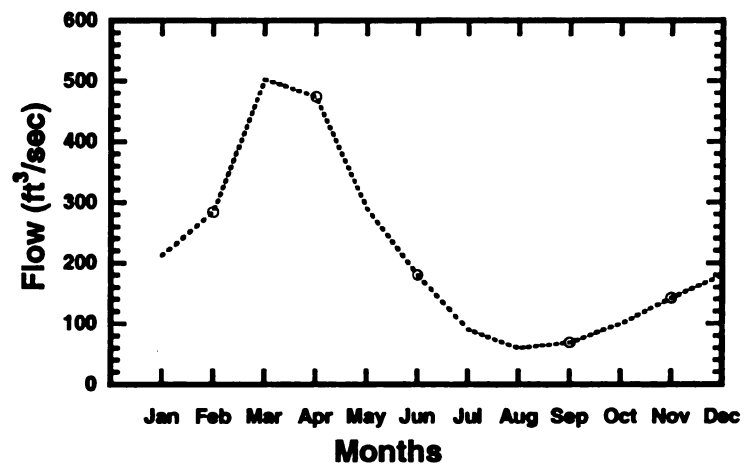


Figure 2-4. Mean monthly stream flow in Red Cedar River for yr 2001.  
(Source:[http://waterdata.sugs.gov/mi/nwis/annual/?site\\_no=04112500&agency\\_cd=USGS](http://waterdata.sugs.gov/mi/nwis/annual/?site_no=04112500&agency_cd=USGS))

### 3. LITERATURE REVIEW

The contaminants or effluents, once discharged into rivers undergo various stages of mixing as they are transported downstream. In broad terms these stages can be classified into two types. In the first stage, commonly referred to as “initial period”, the mixing in the vertical and transverse direction takes place due to turbulence and wall shear. During this period an imbalance exists between advection and turbulent diffusion. The vertical and transverse mixing is quantified by vertical and transverse mixing coefficients respectively both expressed as a function of depth of flow and the bed shear velocity. Fischer (1979) showed however, that the difference in the vertical and lateral dimensions in natural channels makes the transverse mixing coefficient more than 90 times greater than the vertical mixing coefficient, therefore, vertical mixing can safely be assumed to occur instantaneously for a line injection. Nevertheless, determination of transverse mixing coefficient is considered essential in determining the length of stream required for the complete cross-sectional mixing.

The second stage after the cross-sectional mixing is complete is referred to as “Fickian period”. During this stage a balance exists between advection and turbulent diffusion. The most widely used equation to estimate the rates of longitudinal dispersion is the 1-D mass transport equation, more commonly known as 1-D advection-dispersion equation (ADE) i.e.

$$\frac{\partial C}{\partial t} = D_L \frac{\partial^2 C}{\partial x^2} - U \frac{\partial C}{\partial x} \quad (3-1)$$

The analytical solution of this equation for an instantaneous injection of a conservative pollutant is given as:

$$C(x,t) = \frac{M}{2A\sqrt{\pi D_l t}} \exp\left[-\frac{(x-Ut)^2}{4D_l t}\right] \quad (3-2)$$

where:

$C$  = cross-sectionally and vertically averaged concentration

$t$  = time

$D_l$  = longitudinal dispersion coefficient

$x$  = distance in the direction of flow

$U$  = mean longitudinal velocity

$M$  = total mass of the contaminant

For the application of (3-1) the knowledge of an accurate value of dispersion coefficient is necessary. The simplest way is to use a measured dispersion coefficient (Seo and Cheong 1998). In the absence of a tracer test time-concentration data, prediction of the longitudinal dispersion coefficient by other means can be resorted to. In the past few years, the focus has been on the prediction of dispersion coefficients based on the readily available bulk hydraulic parameters i.e., width to depth ratio  $\left[\frac{W}{h}\right]$  and friction

term  $\left[\frac{U}{U_*}\right]$ . Seo and Cheong (1998) developed a new equation by using a combination of

dimensional analysis and regression methods using 59 data sets for 26 rivers in United States to predict the longitudinal dispersion in natural streams. The equation is:

$$\frac{K}{hU^*} = 5.915 \left[ \frac{W}{h} \right]^{0.620} \left[ \frac{U}{U_*} \right]^{1.428} \quad (3-3)$$

where:

$K/hU^*$  = dimensionless dispersion coefficient

$W/h$  = width to depth ratio

$U/U^*$  = friction term defined by  $(8/f)^{1/2}$

$f$  = Darcy- Weisbach's friction factor

Seo and Cheong (1998) also proved that this equation allows for superior predictions as compared to all other existing equations. Deng, et al (2001) proposed a new equation incorporating the effect of transverse mixing and proved that the equation predicts closely in 60.3% of the cases as opposed to 39.7% of the cases by the equation by Seo and Cheong (1998). Their equation is:

$$\frac{K}{hU^*} = \frac{0.15}{8\varepsilon_{i0}} \left[ \frac{W}{h} \right]^{5/3} \left[ \frac{U}{U_*} \right]^2 \quad (3-4)$$

where:

$$\varepsilon_{i0} = 0.145 + \left[ \frac{1}{3250} \right] \left[ \frac{W}{h} \right]^{1.38} \left[ \frac{U}{U_*} \right] \quad (3-5)$$

However the latest development in this area is the equation by Kashefipour and Falconer (2002) who postulated that longitudinal dispersion coefficient is a function of velocity, width and depth of the channel, bed shear velocity, kinematic viscosity and shape factor.



$$D_t = f(U, H, W, U_*, \nu, S_f) \quad (3-6)$$

where:

U= Cross sectional average velocity:

H = Depth of flow

W = Channel width

U<sub>\*</sub>= Bed shear velocity

ν = Kinematic viscosity

S<sub>f</sub>= Shape factor

They argued that, since the flow in natural channels is generally fully turbulent and rough with Reynold's number effects generally being negligible, the kinematic viscosity could be ignored. The approach followed by Kashefipour and Falconer (2002) is essentially the same as that of Seo and Cheong (1998). The new equation proposed was also developed using dimensional analysis and regression for 81 data sets measured in 30 rivers in the US, which is:

$$D_t = 10.612HU \left[ \frac{U}{U_*} \right] \quad (3-7)$$

For 81 data sets, the results predicted by this equation have been reported to be better than those predicted by equations by Seo and Cheong (1998).

Dispersion coefficients are used in the one-dimensional advection-dispersion equation in order to predict concentrations at points downstream. This approach is limited to locations far downstream from the source where the balance between advection and diffusion is achieved (Taylor, 1954). During the “initial period”, advection and diffusion are not balanced and the one-dimensional advection-dispersion equation cannot be applied. Also, due to dominant effect of the velocity distribution during the initial period, the longitudinal distribution of the cross-sectionally averaged concentration is highly skewed, with a steep gradient in the downstream direction and a long tail in the upstream direction. The variance of the longitudinal concentration distribution increases non-linearly with time during the “initial period” and increases linearly with time during the “Fickian period” for a steady uniform flow (Seo and Cheong 1998). For many rivers with irregular boundaries, the process of dispersion is very complicated and many investigators have questioned its characterization by a single coefficient (Seo and Cheong 2001). In the early stages of the transport process, the advective term in eq. (3-1), due to turbulent velocity fluctuations, plays an important role in the diffusion process. As a result, there is an imbalance between the two terms and consequently, the analysis of Taylor (1954) cannot be applied in this section of flow (Kashefipour and Falconer 2002).

The limitation of the “Fickian” model is that it is not able to accurately represent highly skewed concentration profiles often observed in natural streams (Swamee, Pathak et al. 2000). Seo and Cheong (2001) also argue, that the skewness in the time-concentration curves in natural channels is due to the storage zones that retain a portion of solute mass as the main cloud passes by and then the solute is slowly released back into the flow zone.

In cases where time-concentration data is available, an alternative to the one-dimensional advection-dispersion equation has been provided by Swamee et al (2000), in which the calculation of a number of dispersion parameters is suggested rather than relying on a single value of dispersion coefficient. Their model is of the form:

$$c = c_p \left( \frac{t - t_x}{t_p - t_x} \right)^{m-1} \left[ \frac{m+n}{m(n+1)} + \frac{n(m-1)}{m(n+1)} \left( \frac{t - t_x}{t_p - t_x} \right)^{\frac{m}{n}} \right]^{-(n+1)} \quad (3-8)$$

Here,  $m$ ,  $n$ ,  $t_p$ ,  $t_x$  and  $t_d$  are called dispersion parameters. The inception time  $t_x$ , the peak concentration  $C_p$ , and the time of peak concentration  $t_p$  can be readily determined from a time concentration curve. The parameters  $m$  and  $n$  can be determined by plotting  $c/c_p$  against  $(t-t_x)/(t_p-t_x)$  on a double logarithmic plot where  $m-1$  is the slope of the rising limb and  $(m/n + 1)$  is the slope of the recession limb. The optimised values of dispersion parameters are obtained by minimizing the error between the observed concentration profile and the concentration profile predicted by (3-8), which can finally be transformed as the functions of the channel geometry and flow properties for a particular channel geometry. These variables are finally reported in terms of distance from the injection point, flow area, flow velocity and time and are independent of time-concentration data for a subsequent use. Swamee et al (2000) proved that the results from this model are superior when compared to a number of existing predictors.

Davis et al (2000) also presented a solute transport model incorporating the effects of tracer storage in dead zones. They represent stream as consisting of the two parallel regions; the bulk flow region and the dead zone. The bulk flow region occurs in the

central part where the longitudinal dispersive properties are described by one-dimensional advection-dispersion equation, and the dead zone comprises the additional cross-sectional area with slow moving water where tracer can be temporarily stored. They represent exchange between the two regions using first order rate kinetics and the combined shear flow dispersion-dead zone storage model (D-DZM). This provides a much better and physically consistent description of the tracer clouds evolution compared to the conventional one-dimensional advection-dispersion equation. The model is based on the analytical solution of two different equations representing the bulk flow region and the dead zones, which are:

$$\frac{\partial C}{\partial t} + U \frac{\partial C}{\partial x} - K \frac{\partial^2 C}{\partial x^2} = \frac{1}{\chi^2} \frac{\partial C_s}{\partial t} \quad (3-9)$$

$$\frac{\partial C_s}{\partial t} = \frac{\chi^2}{\tau} (C - C_s) \quad (3-10)$$

where:

$\chi = (A/A_s)^{1/2}$  is a relative measure of the effective area of the dead zone region

$\tau$  = characteristic time scale for the exchange of tracer particles between the bulk flow and the dead zones.

Davis et al (2000) obtained the solution of these two equations of the form:

$$C(x,t) = \frac{M}{2A(\pi K t)^{1/2}} \exp\left[-\frac{(x-Ut)^2}{4Kt}\right] e^{-t/\tau} + e^{-x^2/\tau}$$

$$\int_0^t \frac{M}{2A(\pi K v)^{1/2}} \exp\left[-\frac{(x-Uv)^2}{4Kv}\right] e^{x^2/\tau} \frac{\chi}{\tau} e^{-v/\tau} \left(\frac{v}{t-v}\right)^{1/2} I_1\left[\frac{2\chi}{\tau} v^{1/2}(t-v)^{1/2}\right] dv \quad (3-11)$$

where  $v$  is a variable of integration and  $I_1$  is a modified Bessel function of the first kind and first order. This model by also involves obtaining the unknown parameters  $\tau$ ,  $K$  and  $\chi$  by comparing the observed values with those predicted by equation (3-11) and minimizing the error using the least square estimator. They contend that this equation models the decline of peak concentration, growth of variance and overall cloud shape successfully while keeping the parameter values constant or narrow range, thus the dead zone storage accounts for non-Fickian elements in the tracer cloud's evolution.

Seo and Cheong (2001) also follow a similar approach and represent the differential equations for the storage zone and flow zone, which are:

$$\frac{\partial C_f}{\partial t} + U_f \frac{\partial C_f}{\partial x} = k_f \frac{\partial^2 C}{\partial x^2} + \epsilon T^{-1} (C_s - C_f) \quad (3-12)$$

$$\frac{\partial C_s}{\partial t} = T^{-1} (C_f - C_s) \quad (3-13)$$

where:  $C_f$  = flow zone mean concentration

$U_f$  = flow zone mean velocity

$K_f$  = longitudinal dispersion coefficient in the flow zone

$C_s$  = storage zone mean solute concentration

$\epsilon$  = ratio of storage zone area to flow zone area

$T$  = residence time of the tracer in the storage zone =  $A_s/kP$

$A_s$  = cross-sectional area of the storage zone

$P$  = wetted contact length between the flow zone and storage zone in the transverse direction or vertical direction.

$k$  = mass exchange coefficient.

The storage zone model by Seo and Cheong (2001) also is based on evaluating the storage zone parameters by the temporal moments equations derived using moment matching method and equating these to the observed temporal moments calculated from the observed time concentration data. They made use of a robust constrained non-linear equation solver to solve four non-linear equations to evaluate the storage zone parameters. They applied the storage zone model to the measured time- concentration data for the Missouri River and proved that the parameters of storage zone model calculated by using the moment matching method could properly explain the natural dispersion process in the actual streams.

## 4. METHODOLOGY

### 4.1 Selection of Model

Several choices of models are available for use in river-quality planning studies. Following definition of modelling objectives, a thorough review of existing data should be performed. Some important factors which need to be considered in model selection include (1) required accuracy; (2) study timeframe; (3) data availability, attainability and adequacy; (4) availability of the computer program; (5) computational capability; (6) model sophistication; and (7) the availability of source code (Jennings 1976). The appropriate level of model complexity is best addressed by considering the (1) relative costs and problems associated with the model; (2) data availability, and (3) scope of the study being conducted. Since this study is being conducted within the overall framework of Red Cedar River Watershed Project (MSU Water) which is directed at understanding the influence of land use and other campus activities on the water quality of Red Cedar River, it necessitates use of a comprehensive water quality model capable of simulating both the conventional and toxic pollutants.

A number of models like RMA2 (Donnell 1997), RMA4, HSPF, QUAL2EU (Brown and Barnwell Jr. 1987), CE-QUAL-RIVI and DYNHYD/WASP (Ambrose 1993) were considered. Of all the models considered, EPA's hydrodynamic model DYNHYD was selected for the following reasons.

- a. DYNHYD is the driving hydrodynamic model for WASP (water quality analysis simulation program) (Ambrose 1993), which is a generalized modeling

framework for contaminant fate and transport and can be applied in one, two or three dimensions.

- b. WASP is designed to permit easy substitution of user-written sub-routines into the program structure.
- c. WASP consists of two sub models i.e., EUTRO and TOXI, to simulate two major classes of water quality problems.

#### 4.2 Fluorescein As A Water Tracer

For the purpose of this study, the tracer used was fluorescein. Fluorescein is a green dye with a generic name of Acid Yellow 73, which has a colour index of 45350. Maximum excitation and emission for fluorescein occurs at 490 and 520 nm respectively. Fluorescein has a sensitivity of 0.11 micrograms/litre per unit scale and a minimum detectability of 0.29 microgram /litre (Smart and Laidlaw 1977). Its fluorescence is a function of temperature and fluorescence intensity varies inversely with temperature. (Kasnavia and Sabatini 1999). However, preparation of a calibration curve at selected room temperature and analysing all the samples at a constant temperature can overcome this limitation. Another major problem encountered in natural waters is of background fluorescence, which can be due to natural dissolved material and suspended sediments. The level of suspended sediments increases during the spring in Red Cedar with a high discharge due to snow melt, which increases the background fluorescence and reduces effective dye fluorescence due to light absorption and scattering by the suspended particles. Background fluorescence in case of fluorescein is a bigger problem, as it is many times stronger at the green wave band than at the orange. Fluorescence sorbs less as compared to some other fluorescent dyes used in water tracing like rhodamine WT. Red



Cedar River offers a lot of sorption media in terms of weeds, tree branches and suspended solids, hence the use of fluorescein was preferred for this study.

#### 4.3 Model Implementation

The basis for DYNHYD are the equations of continuity and momentum, which are solved for a channel-junction (link-node) computational network. Variable upstream flows and downstream heads drive it. These equations are:

$$\frac{\partial U}{\partial t} - U \frac{\partial U}{\partial x} = -g \frac{\partial H}{\partial x} + \frac{gn^2}{R^{4/3}} U^2 \quad (4-1)$$

$$\frac{\partial A}{\partial t} = - \frac{\partial Q}{\partial x} \quad (4-2)$$

The first term in equation 4-1 is the local acceleration term and denotes rate of change of velocity with time while the second term is the convective inertia term, which represents the rate of momentum change by mass transfer. The first term on right hand side denotes the effect of gravity on the water surface gradient and the last term describes the effects of frictional resistance. The equation of motion (4-1), based on the conservation of momentum predicts water velocities and flows. The equation of continuity (4-2), based on conservation of volume predicts heads and volumes. This approach assumes that the flow is predominantly one-dimensional and accelerations normal to the direction of flow are negligible. Model assumptions include a constant top width, a variable hydraulic depth, and moderate bottom slopes.

The "channel-junction" network solves the equations of motion and continuity at alternating grid points. At each time step, the momentum equation is solved at the channels to compute the velocities, while the heads are obtained by solving the equation of continuity. The time step is selected based on the channel length such that the stability restrictions are satisfied. Typical values of time step used in our computations varied from one to five seconds. The resulting unsteady hydrodynamics are averaged over larger time intervals and are stored for later use by the water quality program (Ambrose 1993). The detailed schematisation of DYNHYD is covered in the user's manual (Ambrose 1988).

#### 4.4 Model Segmentation

Geometric and hydraulic factors as well as the computational considerations are the base, upon which the subdivision of branches into segments is determined (Schaffranek and Goldberg 1981). For the purpose of implementing the St. Venant equations, the entire length of the river in the study section was divided into 103 junctions and 102 channels. Each junction is a volumetric unit acting as receptacle for the water transported through the connecting channels. Taken together all the junctions account for all the water in that portion of the river and the channels account for all the water movement in the river. A 50 meters channel length for each channel was kept so as to conform to the computational stability criteria commonly known as Courant's condition (Ambrose 1993). Ideally the channel lengths should be such that the surface area of the junctions remains close, if not equal, but this requirement was difficult to meet in our case as the channel width varies across the entire reach of the river. Appendix A lists the geometric properties of all the channel and junctions including width, junction surface areas and

direction. Based on these parameters the input file used to run the DYNHYD5 for the given period was prepared which is included in Appendix B.

#### 4.5 Tracer Tests

Hagadorn Road Bridge was selected as the injection site. The three sampling sites selected were Farm Lane Bridge, Kellogg Foot Bridge and Kalamazoo Street Bridge (Figure 2-2). Farm Lane Bridge was selected as a sampling site due to its accessibility and the availability of USGS gage, which would serve as the index gage while Kalamazoo Street Bridge was selected being at the boundary of the river reach under study. The selection of Kellogg Bridge as one of the sampling points was arbitrary just to have an intermediate sampling point at almost middle of the reach. Five tracer tests were conducted for different flow conditions ranging from approximately 2 m<sup>3</sup>/sec to 19 m<sup>3</sup>/sec. Releasing the dye in the middle 75% of the channel width ensured to some extent the conditions of instantaneous mixing. Extensive sampling was done at the three sampling points at the middle of the cross section for the first three dye releases, in which the flow was 16.82 m<sup>3</sup>/sec, 14.41 m<sup>3</sup>/sec and 19.06 m<sup>3</sup>/sec respectively. During the fourth dye release, in which the flow was 2.49 m<sup>3</sup>/sec, sampling could only be done at Bogue Bridge located upstream of the first sampling point, due to extremely low velocity (Figure 2-2), however, three different points across a transect could be sampled to ascertain if complete transverse mixing has been reached. For the fifth dye release, sampling was only done at Farm Lane Bridge and Kalamazoo Bridge only and sampling at Kellogg Bridge had to be omitted due to long sampling interval at each sampling station.

Fluorescein solution with a concentration of 179.06 grams per litre was used for all the tracer tests in order to have a consistency. The volume of the dye used was based on a desired peak concentration range of 10-20 micrograms/litre at the last sampling point located at a distance of 5.079 kilometres from the release point.

#### 4.6 Data Collection.

Collection and analysis of surface water data and information is a complex task. A variety of instruments, measurement methods and analytical techniques are usually required to produce a surface water record for a single site. Three comprehensive sets of data are required to carry out flow simulations by mathematical models such as the branch-network flow model. Initial condition data, channel geometry data and boundary-value data constitute mandatory data requirements for flow computation by the branch channel network flow model (Schaffranek and Goldberg 1981).

This study focused on recommended methods for data gathering and field measurements in order to ensure data comparability with the data acquired by other federal agencies like USGS. The Mid-section method as outlined in National Handbook of recommended methods for Water Data Acquisition (1977) was used to calculate the cross-sectional areas and discharges. Also a two-point method was employed to measure the velocities at different cross sections. Field measurement at Library Bridge and Kellogg Bridge was done for eight consecutive days from 04 April 2002 to 11 April 2002. The field data collected for the purpose of this study were:

- a. Stage measurements at the downstream boundary (Kalamazoo street Bridge) to generate head versus time as one boundary condition of the model.

- b. Discharge measurements at Hagadorn Bridge as one of the model inputs at the first junction. Farm Lane gage is located 1400 meters downstream of the inlet boundary at Hagadorn Bridge, therefore the discharge measurements available from USGS gage at the Farm Lane Bridge were extrapolated in terms of time to yield the values for discharge at Hagadorn Bridge.
- c. Velocity and stage measurements at, Library Bridge and Kellogg Foot Bridge for calibration of the model. These measurements were made using a Gurley Precision price AA current meter and USGS bridge board set. The field data collected is summarized in Appendix C.

#### 4.7 Manning's Roughness Coefficient.

Calculation of stream discharge and floodwater elevations requires the evaluation of flow impeding characteristics of the stream channels and their banks. Manning's roughness coefficient is commonly used to assign a quantitative value to represent the collective effect of these characteristics. In DYNHYD5, it acts as a tuning knob to calibrate the model. Changing the value of "Manning's n" in one channel affects the upstream and downstream channels. Increasing the value of "Manning's n" causes more energy to be dissipated in that channel. As a result, the velocity head will decrease and time of travel in that channel will increase. Lowering "Manning's n" will decrease resistance to flow, resulting in a higher velocity head and a shorter time of travel.

The user's manual for DYNHYD gives a generalized value of "Manning's n" between 0.01-0.08. However Coon (1998) suggests a value of "Manning's n" as 0.035-0.100 for major streams with a top width greater than 100 ft at flood stage and with

irregular and rough section. Nevertheless it is mostly the velocities, which are more sensitive to “Manning’s  $n$ ” values as compared to water surface elevations or discharges.

## 5. RESULTS AND DISCUSSION

### 5.1 Model Calibration

The head, velocity and discharge measured from 4 April 02 to 11 April 02 at the Library and Kellogg bridges were used to calibrate the model. Calculation of stream discharge and floodwater elevations requires the evaluation of flow impeding characteristics of the stream channels and their banks. Manning's roughness coefficient is commonly used to assign a quantitative value to represent the collective effect of these characteristics. In DYNHYD5, it acts as a tuning knob to calibrate the model. Changing the value of "Manning's  $n$ " in one channel affects the upstream and downstream channels. Increasing the value of "Manning's  $n$ " causes more energy to be dissipated in that channel. As a result, the velocity head will decrease and time of travel in that channel will increase. Lowering "Manning's  $n$ " will decrease resistance to flow, resulting in a higher velocity head and a shorter time of travel.

The major factors affecting the roughness coefficient are size, shape and distribution of grain size material, channel surface irregularity, channel shape variation, obstructions, type and density of vegetation and degree of meandering. Nevertheless it is mostly the velocities, which are more sensitive to "Manning's  $n$ " values as compared to water surface elevations or discharges. A range of 0.035 to 0.10 for major streams with a top width at flood stage greater than 30 meters for an irregular and rough section has been proposed by Chow (1959). For DYNHYD 5, a value of roughness coefficient for each channel is required as a model input data. Most of the empirical equations used to calculate " $n$ " are based on the size of the bed material, for which no comprehensive data existed for this reach. Therefore, Manning's roughness coefficient values for each

channel were estimated basing on an empirical equation by V.B Sauer (Coon 1998). With this equation, it is possible to calculate the roughness coefficient using the hydraulic radius and the water surface elevations. The equation is:

$$n = 0.11S_w^{0.18}R^{0.08} \quad (5-1)$$

where:

$S_w$  = slope of water surface in meter/meter

$R$  = hydraulic radius in meters

Basing upon this equation, following values were calculated for Manning's roughness coefficient.

Table 5-1 Manning's Roughness Coefficients

Channel Number	Manning's Roughness Coefficient
1-17	0.021
18-27	0.032
28-38	0.036
39-45	0.022
46-62	0.031
63-68	0.036
69-102	0.031



## 5.2 Hydrodynamics

The velocities, heads and flows predicted by the model at the library bridge were generally consistent and in agreement with the observed values for all type of flow conditions (Figure 5-1) to (Figure 5-3) although an under prediction of the velocities was observed for flow lower than 14 m<sup>3</sup>/sec. At Kellogg Bridge the flows predicted by DYNHYD are in general agreement with the measured flows, however the velocities were higher than the measured velocities and the heads were less than the measured values (Figure 5-4) to (Figure 5-6).

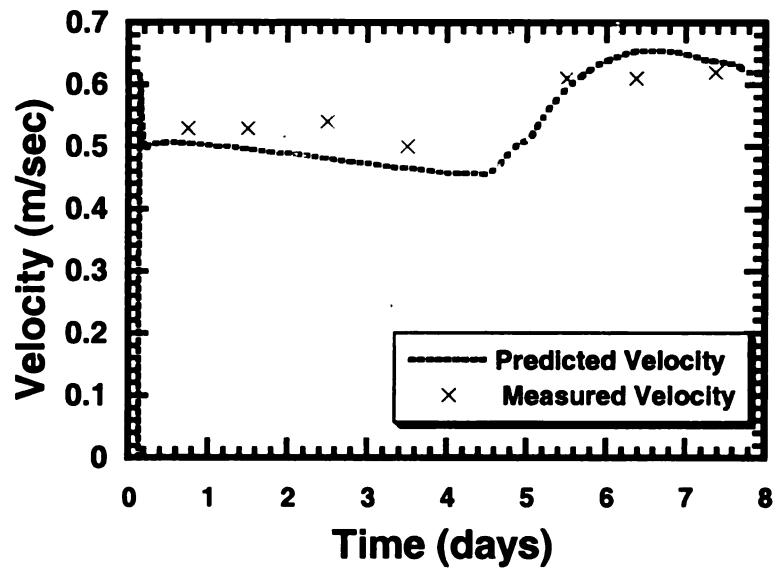


Figure 5-1. Predicted and measured velocity at Library Bridge (4-11 April, 02).

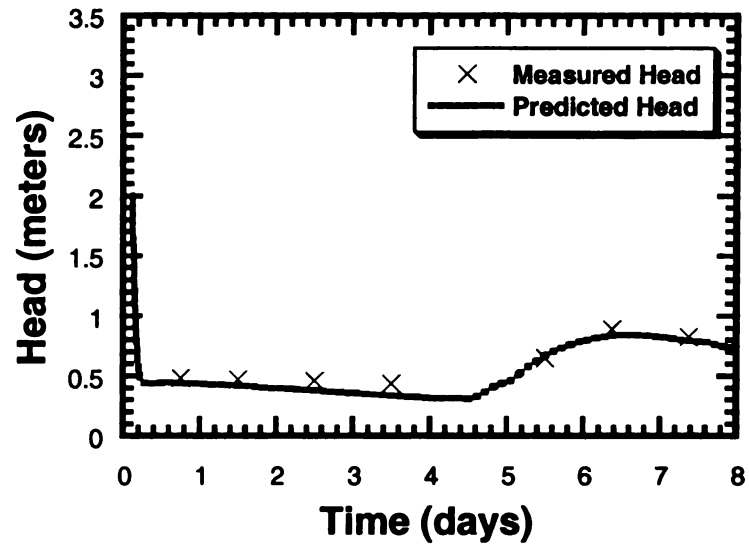


Figure 5-2. Predicted and measured head at Library Bridge (4-11 April, 02).

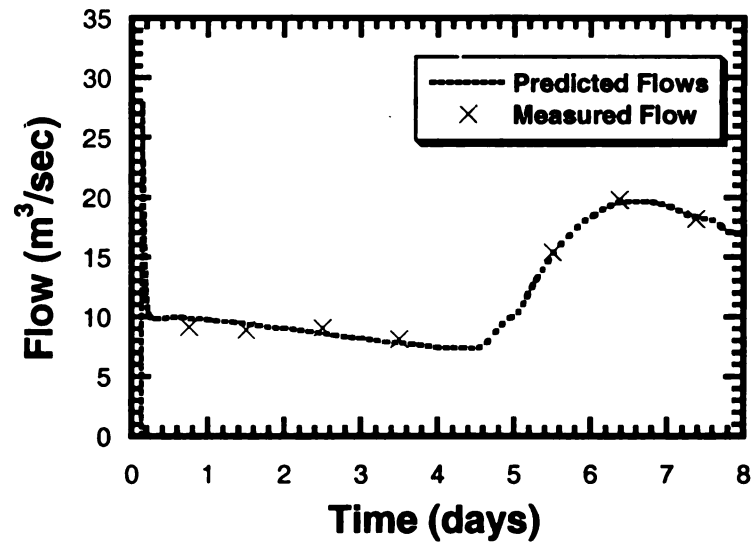


Figure 5-3. Predicted and measured flow at Library Bridge (4-11 April, 02).

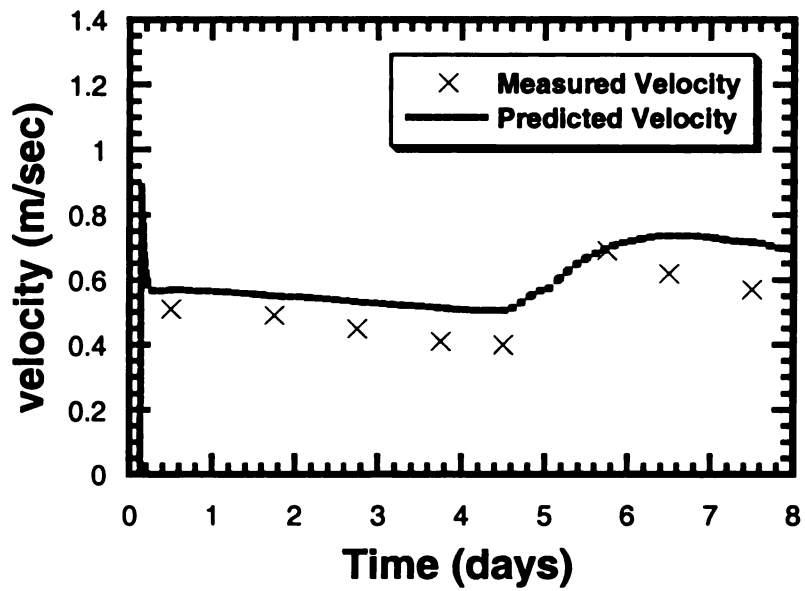


Figure 5-4. Predicted and measured velocity at Kellogg Bridge (4-11 April, 02).

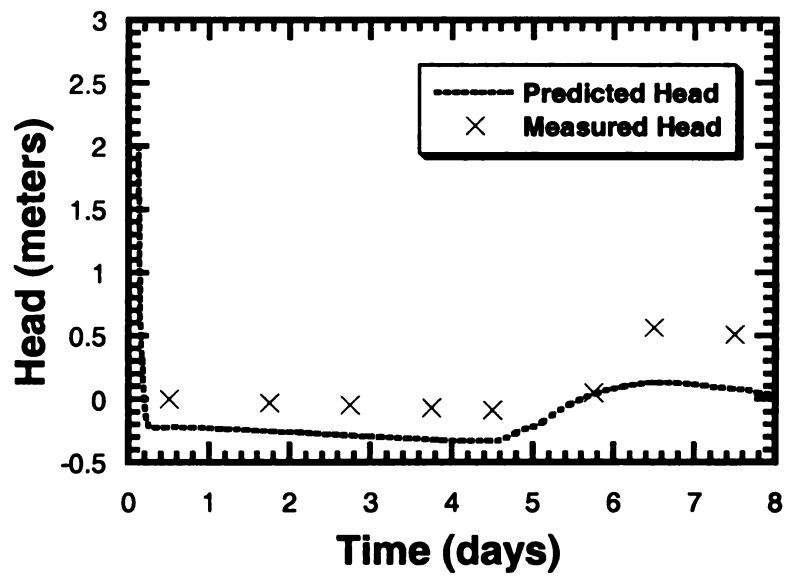


Figure 5-5. Predicted and measured head at Kellogg Bridge (4-11 April, 02)

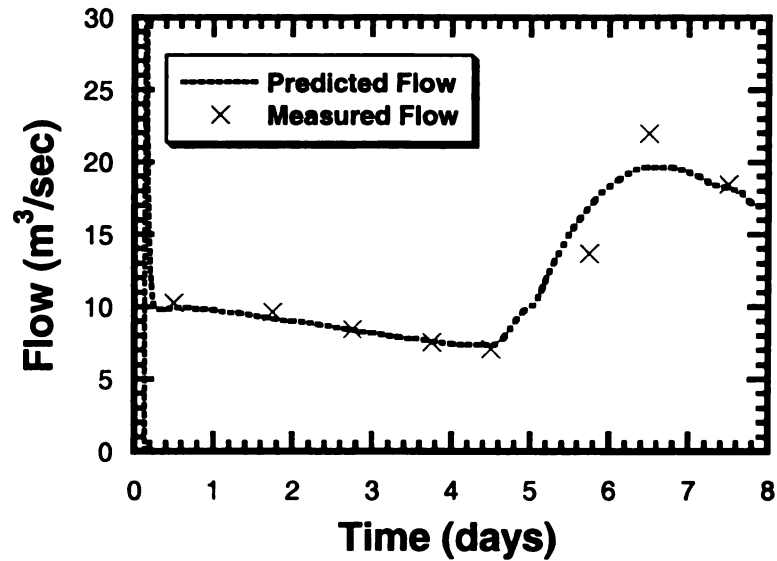


Figure 5-6. Predicted and measured flow at Kellogg Bridge (4-11 April, 02).

No specific guidance criteria for the error statistics for calibrating the hydrodynamic model for a natural stream could be found in the literature, therefore the preliminary guidance criteria by (Wu 1995) for estuarine water quality models was taken as a guideline. According to these criteria, the correlation coefficient should be greater than 0.94 for hydrodynamic variables, 0.84 for transport of a conservative water quality variable and 0.60 for water quality variables. Comparison of model predictions and observed data was performed using linear regression techniques (Thoman 1982). Three standard linear regression statistics were computed which are (1) square of the correlation coefficient (2) slope of the regression line and (3) intercept of the regression line. The slope of the regression line represents how well trends can be projected with the calibrated model and the intercept indicates if any systematic error is present. The square of correlation coefficient for all the hydrodynamic variables i.e., velocity, head and discharge was calculated between 0.918 to 0.992 at the Library Bridge and 0.718 to 0.90

for the Kellogg Bridge respectively. Also, the root mean square error (RMSE), which is the mean square of any residuals, is also a useable statistics to verify model forecasts, and is applicable to a large number of analysis and forecast elements. The smaller the RMSE, the better is the performance of the model. The regression analysis figures are tabulated in (Table 5-2).

Table 5-2. Regression statistics for hydrodynamic variables.

Parameter	Library Bridge			Kellogg Bridge		
	Velocity	Head	Flow	Velocity	Head	Flow
$R^2$	0.916	0.97	0.99	0.83	0.78	0.92
Slope	0.594	0.894	1.009	0.967	1.22	1.014
Intercept	0.237	0.106	-0.151	-0.064	0.289	-0.187
RMSE	0.0358	0.060	0.414	0.093	0.285	1.426

The velocity and head predicted by the model at the Kellogg Bridge were not as close to the observed values as was the case for the Library Bridge. This could not be improved by grid refinement. The sharp bend just before the Kellogg Bridge appears to have an influence on the velocities, which could not be accurately captured by the model.

### 5.3 Effect of Grid On Model Performance

As described earlier, the entire reach needed to be divided into number of channels (segments) for the implementation of computational scheme on a network. Different grids were tried and implemented. Three different grids comprising 28 channels, 102 channels and 153 channels were tested. For 28-channel grid, the mean length to width ratio was 7.5, with a maximum of 12.3 and minimum of 3.7. For the 102-channel grid, a constant

segment length of 50 meters was tested, for which the max, min and mean length to width ratios were 3.06, 1.24 and 1.85 respectively. For 153-channel-grid, a constant length to width ratio of 1.2 was tried. Although the refinement of the model grid from 28 channels to 102 channels refined the model output, further refinement of the grid to 153 channels made the model predictions worse. This is likely related to a violation of the channel length requirement in DYNHYD for some of the channels (Ambrose 1993), according to which:

$$\Delta x_i \geq (\sqrt{gH_i} \pm U_i) \Delta t$$

where:

$\Delta x_i$  = length of channel  $i$ , m

$H_i$  = mean depth of channel  $i$ , m

$U_i$  = velocity in channel  $i$ , m

$\Delta t$  = computational time step

$g$  = acceleration due to gravity

This also reduced the time step to almost 1 second thereby increasing the run time by several orders. Also, the max river width is 40.2 meters, which entails that the longitudinal dimension for a segment must be greater than this value in order to prevent masking of the velocity profile in the longitudinal direction.

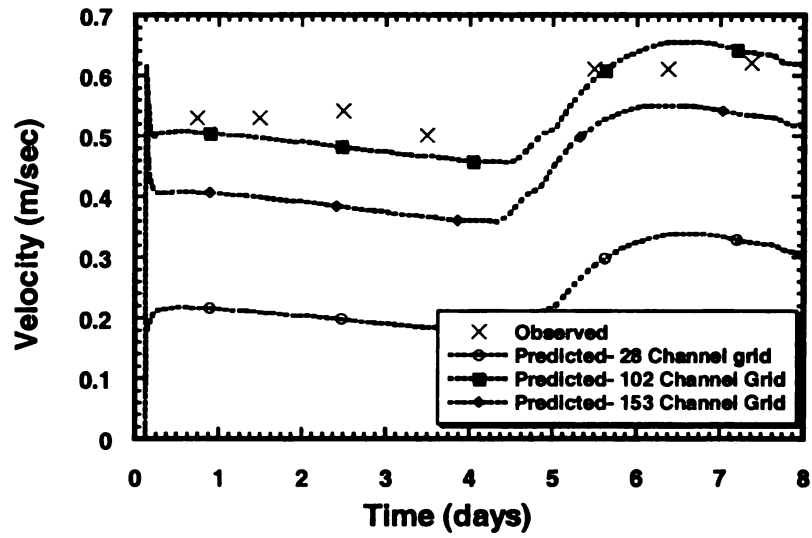


Figure 5-7. Effect of different grids on predicted velocity at the Library Bridge.

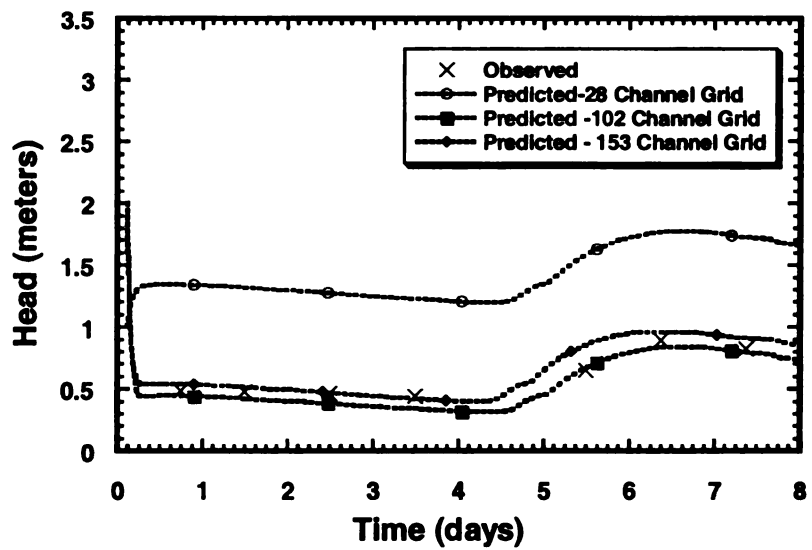


Figure 5-8. Effect of different grids on predicted head at the Library Bridge.

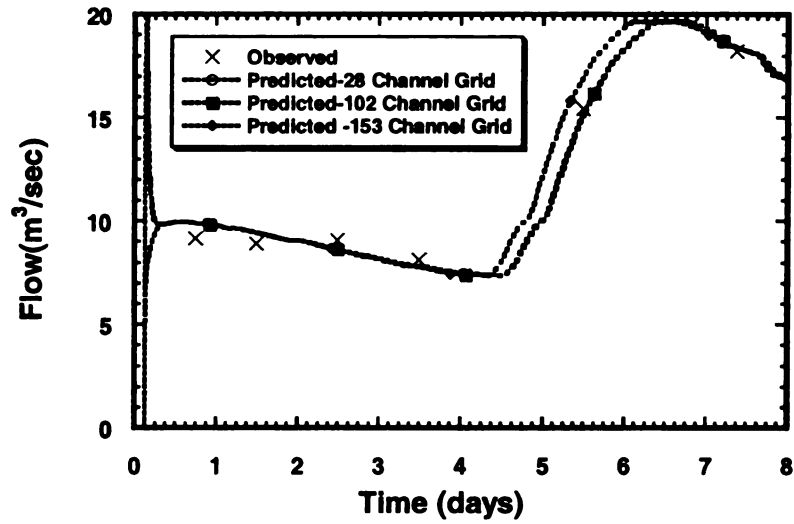


Figure 5-9. Effect of grid on predicted flow at the Library Bridge.

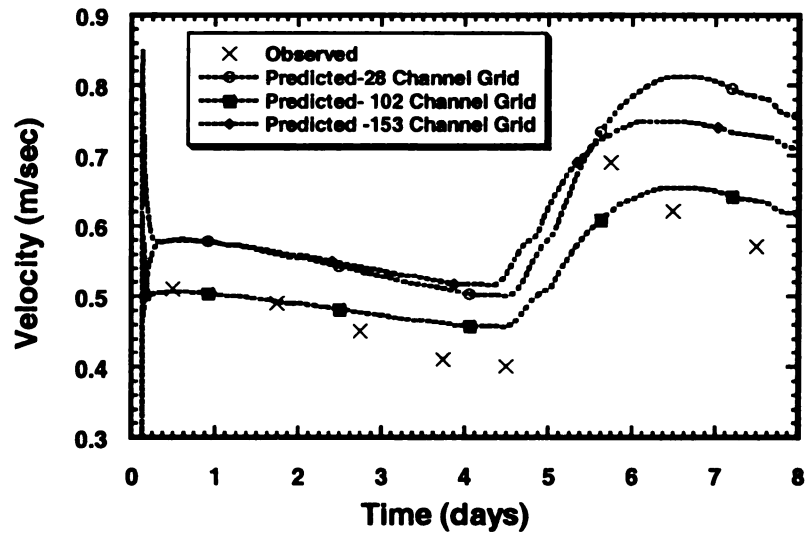


Figure 5-10. Effect of different grids on predicted velocity at the Kellogg Bridge.



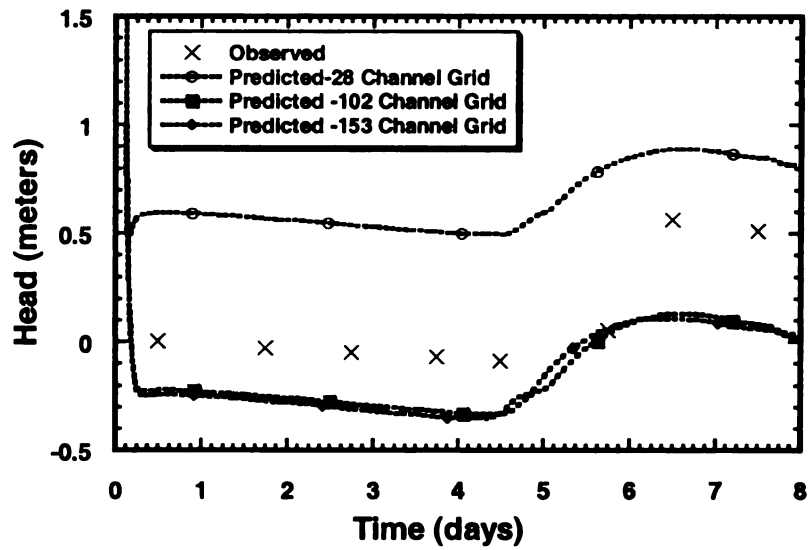


Figure 5-11. Effect of different grids on predicted head at the Kellogg Bridge.

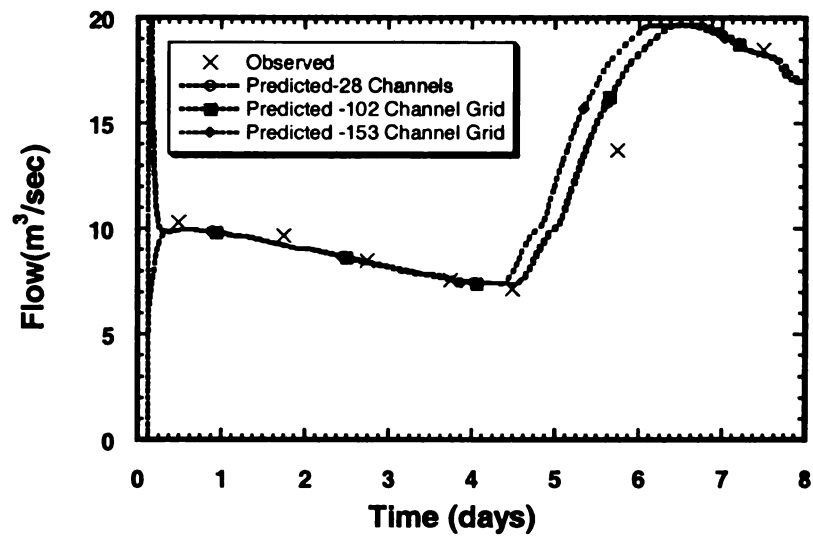


Figure 5-12. Effect of different grids on predicted flow at the Kellogg Bridge.

#### 5.4 Effect of Time Step on Model Performance

For a fixed length, as in this case, the Courant condition restricts the time increment of the solutions accordingly, (Schaffranek and Goldberg 1981), i.e.

$$\Delta t \leq \frac{\Delta x_i}{|U_i \pm \sqrt{gH_i}|} \quad (5-2)$$

According to Schaffranek and Goldberg (1981), although the time step to segment length ratio presented by Courant condition need not to be strictly upheld, the conservative properties of the model, and hence the accuracy of the results, are the best values close to the courant criterion. As per this condition, the value of the time step calculated was close to 10 seconds using a constant segment length of 50 meters, the maximum reach velocity of 0.7 m/sec, and maximum reach depth of 2 meters. However the model became unstable for a time step of 7 seconds and above. Also the model runs for different time steps within the stable range of 1, 2, 3, 4 and 5 seconds showed no dispersion of the results as can be seen in (Figure 5-13) through (Figure 5-16), in which the simulated parameter values for all the different time steps is exactly the same.

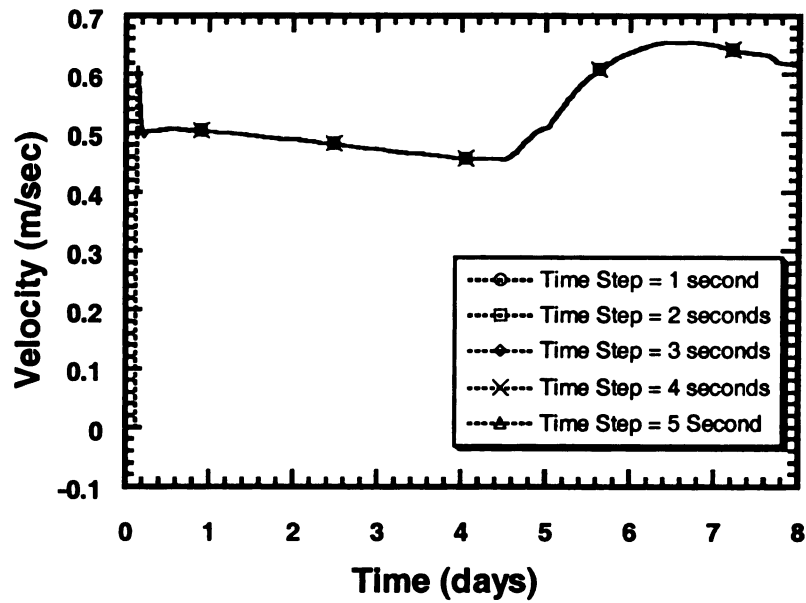


Figure 5-13. Effect of different time step size on predicted velocity at Library Bridge.

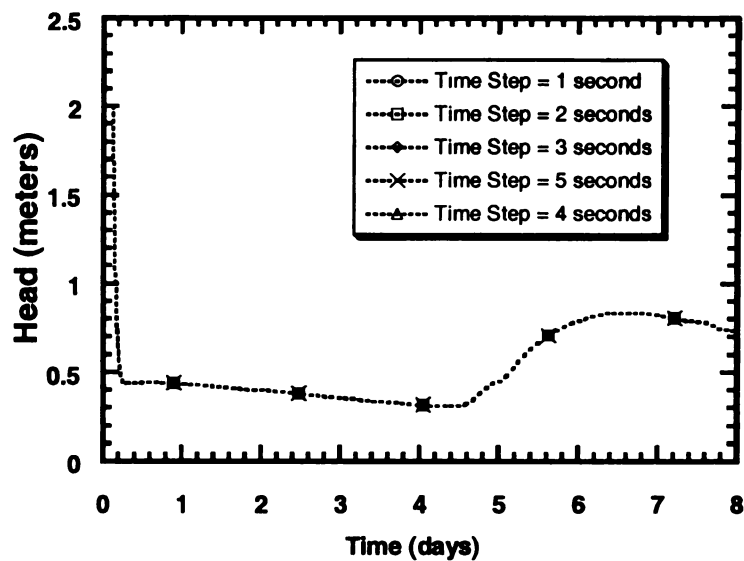


Figure 5-14. Effect of different time step size on predicted head at Library Bridge

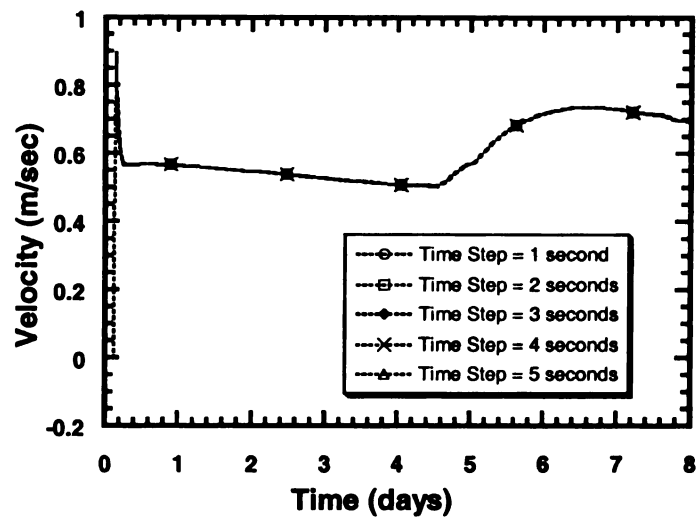


Figure 5-15. Effect of different time step size on predicted velocity at Kellogg Bridge.

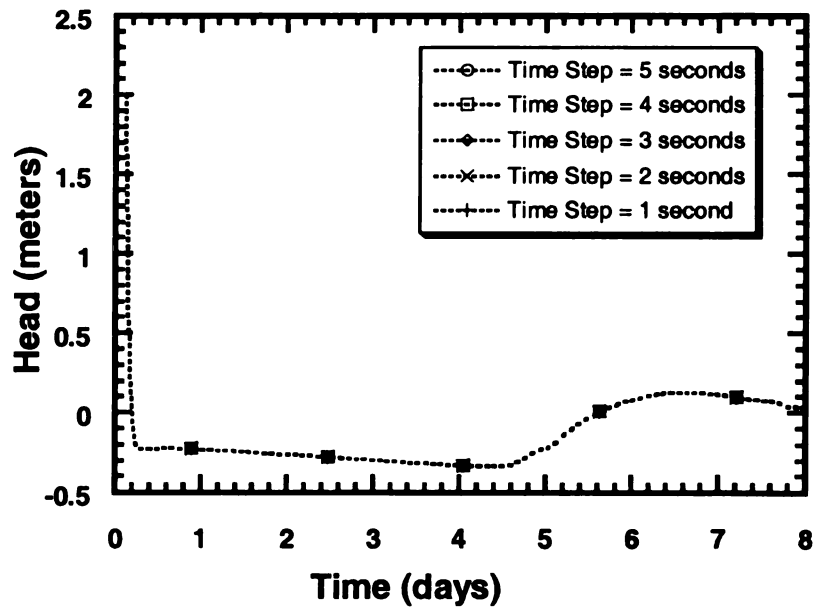


Figure 5-16. Effect of different time step size on predicted head at Kellogg Bridge.

## 5.5 Time of Travel

The sampling schedule for each dye study depended on the flow but the sampling interval was between 1–4 minutes at all sampling points. The time-concentration data for 5 dye releases is presented in **Appendix D** through **Appendix H** and the time concentration plots are presented in Figure 5-17 through Figure 5-21 for each dye release. The time of arrival of the leading edge, peak, centroid and the trailing edge at each sampling sites are presented in Table (5-3) through (Table 5-7).

Table 5-3. Time of travel data-dye release 1 (May 17, 2002).

Sampling Location	Distance From Injection Point (Km)	Leading Edge	Peak	Centroid	Trailing Edge	Discharge at Index Gage (m <sup>3</sup> /sec)	Peak Conc. C <sub>p</sub> (ug/L)	Time of passage of dye cloud (mins)
		Travel Time (mins)	Travel Time (mins)	Travel Time (mins)	Travel Time (mins)			
Farm Lane Bridge	1.4	46.15	59.15	63.57	86.17	16.82	41	40.02
Kellogg Bridge	3.1	99	113.09	125.22	163	17.1	17.9	64
Kalamazoo Bridge	5.079	146.88	175.72	181.76	274	17.1	15.4	127.12

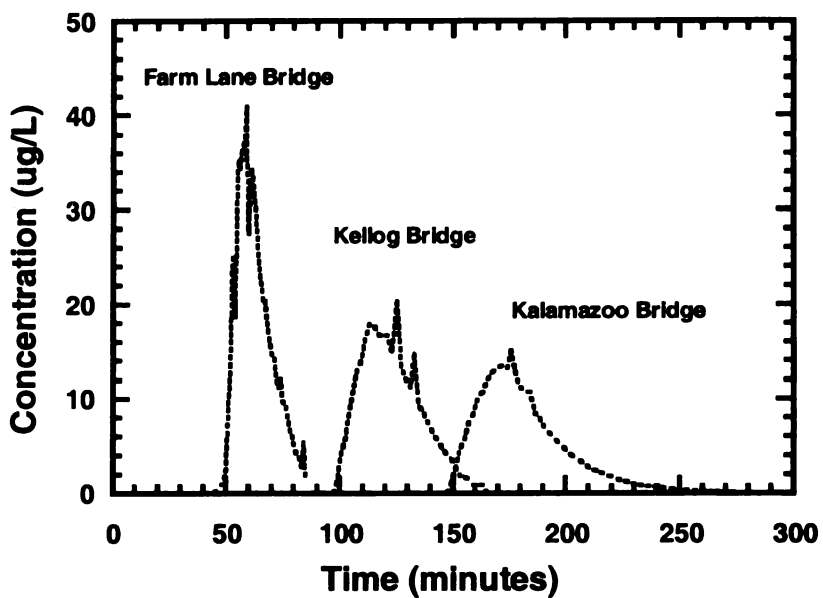


Figure 5-17. Time-concentration curves-dye release 1 (May 17, 2002).

Table 5-4. Time of travel data-dye release 2 (May 31, 2002).

Sampling Location	Distance From Injection Point (Km)	Leading Edge	Peak	Centroid	Trailing Edge	Discharge at Index gage (m <sup>3</sup> /sec)	Peak Conc. C <sub>p</sub> (ug/L)	Time of passage of dye cloud (mins)
		Travel Time (mins)	Travel Time (mins)	Travel Time (mins)	Travel Time (mins)			
Farm Lane Bridge	1.4	54	62	70	98	14.41	86.8	44
Kellogg Bridge	3.1	109	125	135	174	14.16	36	65
Kalamazoo Bridge	5.079	154	192	204	307	14.01	26.8	153

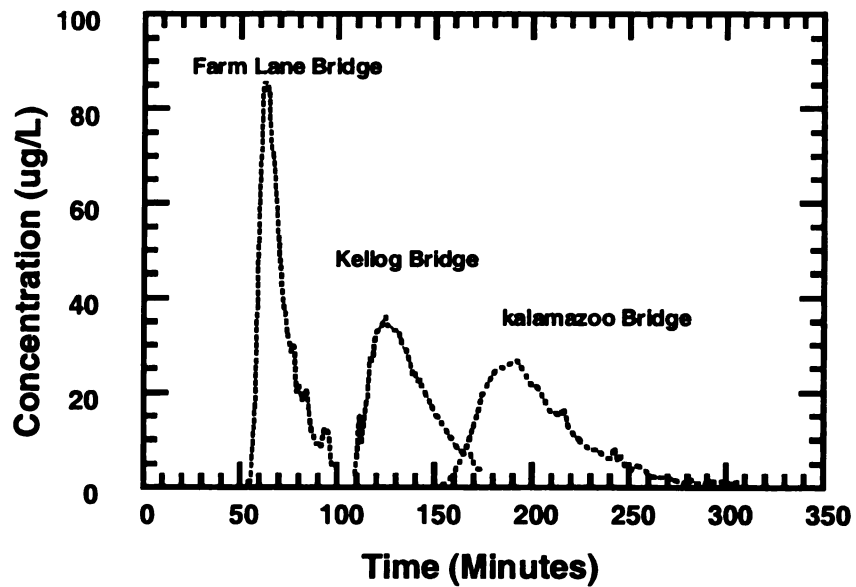


Figure 5-18. Time-concentration curves-dye release 2 (May 31, 2002).

Table 5-5. Time of travel data-dye release 3 (Jun 6, 2002).

Sampling Location	Distance From Injection Point (Km)	Leading Edge	Peak	Centroid	Trailing Edge	Discharge at Index gage (m <sup>3</sup> /sec)	Peak Conc. C <sub>p</sub> (ug/L)	Time of passage of dye cloud (mins)
		Travel Time (mins)	Travel Time (mins)	Travel Time (mins)	Travel Time (mins)			
Farm Lane Bridge	1.4	42	52	64.00	99	19.06	79.6	57
Kellogg Bridge	3.1	91	106	118.00	175	18.77	36.8	84
Kalamazoo Bridge	5.079	118	163	176.00	289	18.35	28.4	171

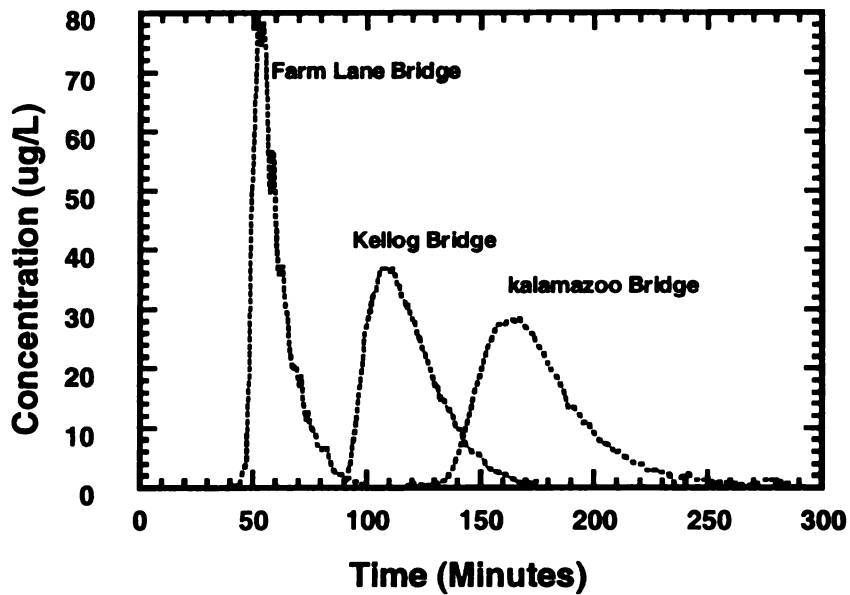


Figure 5-19. Time-concentration curves-dye release 3 (Jun 6, 2002).



Table 5-6. Time of travel data-dye release 4 (Jun 21, 2002).

Sampling Location	Distance From Injection Point (Km)	Leading Edge	Peak	Trailing Edge	Discharge at Index gage (m <sup>3</sup> /sec))	Peak Conc. C <sub>p</sub> (ug/L)	Time of Passage of Dye Cloud (mins)
		Travel Time (mins)	Travel Time (mins)	Travel Time (mins)			
(Left)	0.865	129	156	287	2.492	52	158
(Centre)	0.865	129	153	209	2.492	71.6	80
(Right)	0.865	133	155	241	2.492	65.1	108

Note: - The timings for the trailing edge are based upon extrapolated values up to 10% of the peak concentrations observed. These samples were taken at Bogue Bridge located at 850 meters downstream of injection point at Hagadorn Bridge

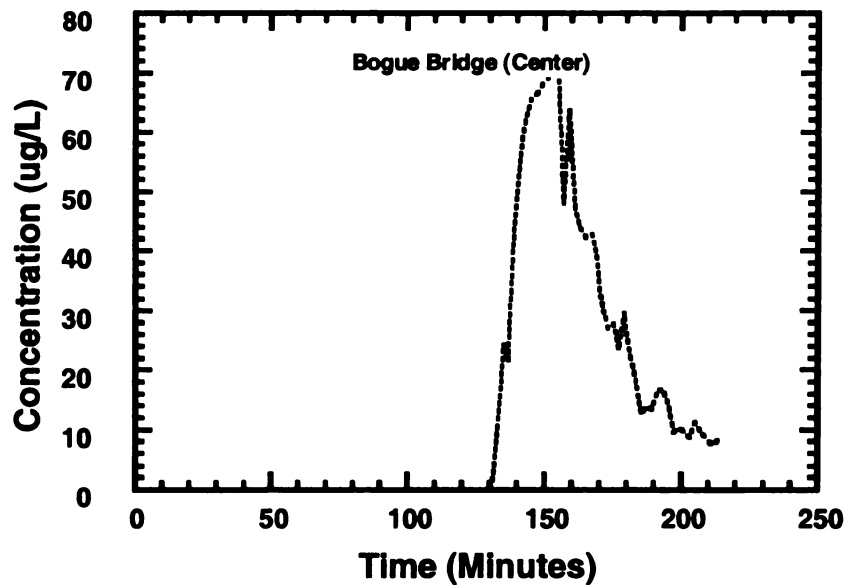


Figure 5-20. Time-concentration curve-dye release 4 (Jun 21, 2002).

Table 5-7. Time of travel data-dye release 5 (Jun 25, 2002).

Sampling Location	Distance From Injection Point (Km)	Leading Edge	Peak	Trailing Edge	Discharge at Index gage (m <sup>3</sup> /sec)	Peak Conc. C <sub>p</sub> (ug/L)	Time of passage of dye cloud (mins)
		Travel Time (mins)	Travel Time (mins)	Travel Time (mins)			
Farm Lane Bridge	1.4	271	309	453	2.06	15.8	182
Kalamazoo Bridge	5.079	588	768	NA	2.06	4.7	NA

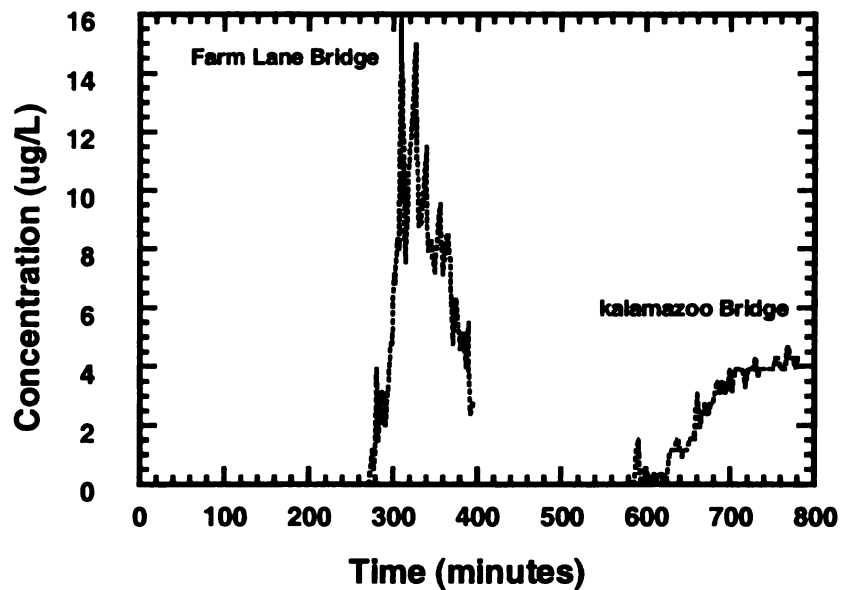


Figure 5-21. Time-concentration curves-dye release 5 (Jun 25, 2002).

The time taken by the leading edge and the peak of the dye cloud showed a consistent trend at  $16.82\text{ m}^3/\text{sec}$ ,  $14.41\text{ m}^3/\text{sec}$  and  $19.06\text{ m}^3/\text{sec}$  flows, however the trailing edge deviated from the trend at Kellogg Bridge for a flow of  $19.06\text{ m}^3/\text{sec}$  (Figure 5-22) to (Figure 5-24). At a flow of  $2.49\text{ m}^3/\text{sec}$  the leading edge reached the Farm Lane Bridge 271 minutes after the dye injection as compared to 54, 46 and 42 minutes for  $14.41\text{ m}^3/\text{sec}$ ,  $16.82\text{ m}^3/\text{sec}$   $19.06\text{ m}^3/\text{sec}$  flows respectively. The extraordinarily long time taken by the leading edge to reach Farm Lane at low flow conditions can be attributed to the upward slope in the river reach between Farm Lane and Hagadorn Bridge, which retards the water movement in the absence of inertia due to low volume of flow. A similar trend was observed for the peak of the dye cloud at low flow. The time to peak concentration at Farm Lane was 309 minutes against 62, 59 and 52 minutes at  $14.41\text{ m}^3/\text{sec}$ ,  $16.82\text{ m}^3/\text{sec}$   $19.06\text{ m}^3/\text{sec}$  flows respectively. The steep slope of the lines from  $2.06\text{ m}^3/\text{sec}$  to  $14.41\text{ m}^3/\text{sec}$  is indicative of non-linearity in the trend for low flow conditions. However for the medium flow range, the change in the arrival time for leading edge, peak and the trailing edge is not considerable. The possible reasons for the skewness in the trailing edge could be adsorption and desorption, transient storage or any other process, which so far cannot be explained by the available data.

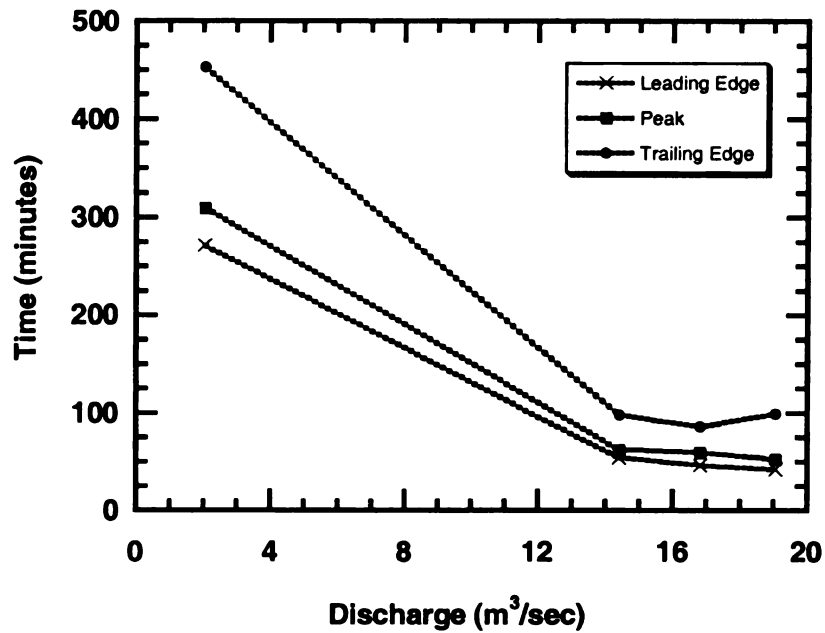


Figure 5-22. Time of arrival of leading edge, peak and trailing edge of the dye cloud at Farm Lane Bridge for different flow conditions.

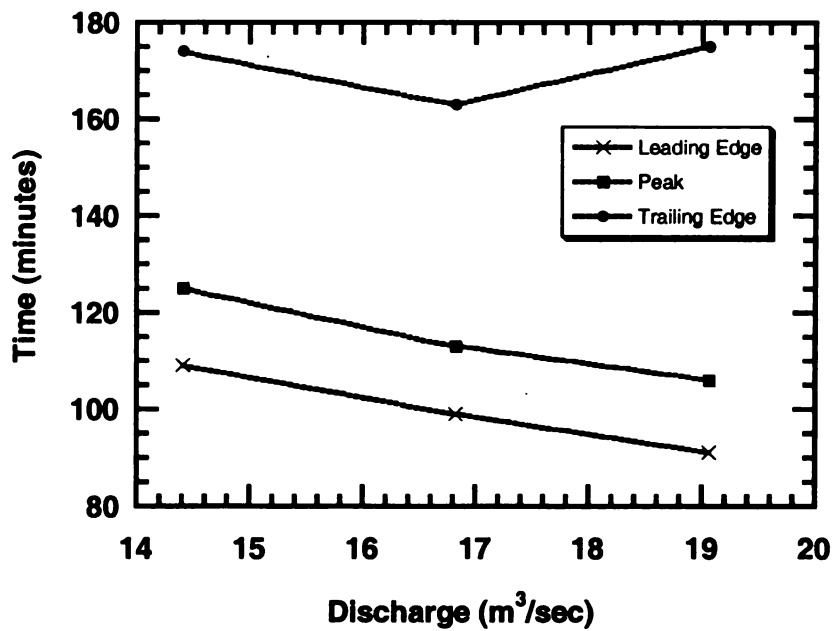


Figure 5-23. Time of arrival of leading edge, peak and trailing edge of the dye cloud at Kellogg Bridge for different flow conditions.

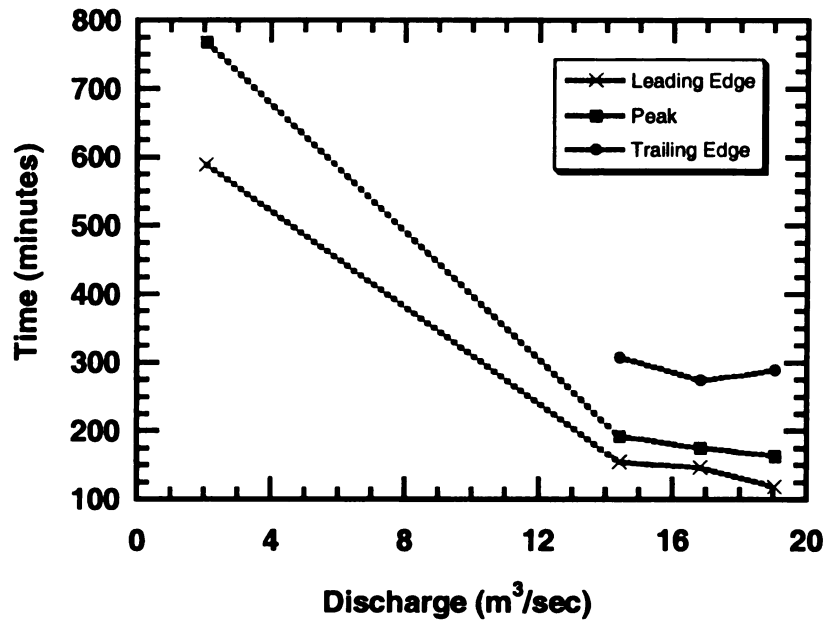


Figure 5-24. Time of arrival of leading edge, peak and trailing edge of the dye cloud at Kalamazoo Bridge for different flow conditions.

## 5.6 Dispersion by Moments Method

Two different methods were used to calculate the dispersion coefficients i.e. method of moments given by Fischer (1968) by using the time concentration data at an upstream and a down stream location and mass transport. The method of moments takes into account the spread of the dye cloud about the centroid as it moves from one sampling point to the second sampling point and hence entails a minimum of two data points to calculate the dispersion in a given reach. By this method the dispersion coefficient is given by:

$$D_x = \frac{U^2}{2} \frac{\sigma_{td}^2 - \sigma_{tu}^2}{t_d - t_u} \quad (5-3)$$

where: -

$D_x$  = dispersion Coefficient

$U^2$  = reach average mean velocity

$t_d, t_u$  = downstream and upstream mean time

$\sigma^2$  = variance of the time concentration curve (extrapolated to 1% of the peak dye concentration).

The mean time and the variance are calculated using the time-concentration data by following integrals:

$$t = \frac{\sum_{i=0}^{n-1} (c_i t_i + c_{i+1} t_{i+1}) (t_{i+1} - t_i)}{\sum_{i=0}^{n-1} (c_i + c_{i+1}) (t_{i+1} - t_i)} \quad (5-4)$$

$$\sigma^2 = \frac{\sum_{i=0}^{n-1} [c_i (t_i)^2 + c_{i+1} (t_{i+1})^2] (t_{i+1} - t_i)}{\sum_{i=0}^{n-1} (c_i + c_{i+1}) (t_{i+1} - t_i)} - t^2 \quad (5-5)$$

The time concentration data sets for the first and third sampling points were used to calculate the reach averaged dispersion coefficients being better representative of the entire reach for a flow of 14.41 m<sup>3</sup>/sec, 16.82 m<sup>3</sup>/sec and 19.06 m<sup>3</sup>/sec. The dispersion coefficients for the low flow conditions couldn't be calculated due to incomplete trailing edge at Kalamazoo Bridge. The values of dispersion coefficients are presented in Table 5-8.

Table 5-8 Dispersion Coefficients By Moments Method

Flow	Velocity	Dispersion Coefficient
m <sup>3</sup> /sec	m/sec	m <sup>2</sup> /sec
14.41	0.459	33.3
16.82	0.52	25.24
19.06	0.545	41.4

However, the value of dispersion coefficient for a flow of 16.82 m<sup>3</sup>/sec was recalculated as 37.49 m<sup>2</sup>/sec by interpolating the values for 14.41 m<sup>3</sup>/sec and 19.06 m<sup>3</sup>/sec because the trailing edge at Kalamazoo for a flow of 16.82 m<sup>3</sup>/sec was missed during sampling.

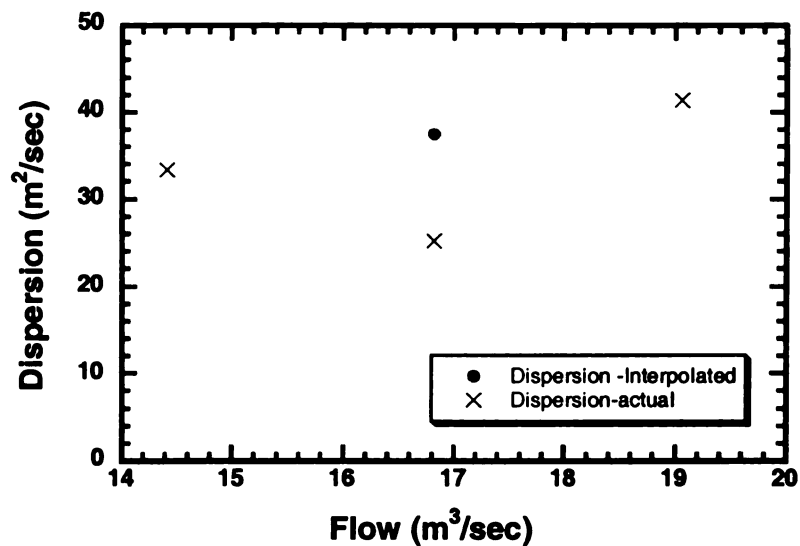


Figure 5-25. Dispersion coefficients calculated using moments method for medium flow conditions.

## 5.7 Dispersion By Mass Transport

The concentrations of a contaminant can also be determined by mass transport equation (Thomann and Muller 1987) at a distance “x” downstream at any instant of time. The equation is:

$$C(x,t) = \left[ \frac{M}{2A\sqrt{\pi D_x t}} \right] \exp \left[ \frac{-(x-Ut)^2}{4D_x t} - Kt \right] \quad (5-6)$$

where:

$C$  = average cross section concentration

$x$  = distance from injection point to sampling point

$t$  = elapsed time

$D_x$  = longitudinal dispersion coefficient

$A$  = average cross sectional area

$M$  = total mass of the contaminant

$U$  = average flow velocity

$K$  = decay coefficient

A rearranged form of mass transport equation calculates the dispersion based upon the peak concentration and the time of peak concentration at the sampling point.



$$D_x = \left[ \frac{M}{2AC_p \sqrt{\pi T_p}} \right]^2 \quad (5-7)$$

Therefore the dispersion can be calculated even by measuring the concentrations at one location within the given reach. But the variability in the geometric configuration of the channel necessitates sampling at greater number of points to yield better relationships of dispersion with respect to distance on different flow conditions. The dispersion coefficients at different flow conditions calculated using the above equation are listed in Table (5-9).

Table 5-9 Dispersion coefficients calculated using the mass transport equation.

Location	Distance From Injection Point (km)	Dispersion Coefficient at Various Flow conditions (m <sup>2</sup> /sec)			
		2.06 m <sup>3</sup> /sec	14.41 m <sup>3</sup> /sec	16.82 m <sup>3</sup> /sec	19.06 m <sup>3</sup> /sec
Farm Lane Bridge	1.4	0.74	1.55	1.65	2.58
Kellogg Foot Bridge	3.2	Not Available	5.96	6.27	7.66
Kalamazoo Bridge	5.079	7.13	7.63	5.69	9.33

Generally the dispersion coefficients calculated by mass transport equation showed consistent trends. The dispersion increased with an increase in flow (Figure 5-26). The dispersion value of 5.69 m<sup>2</sup>/sec at a flow of 16.82 m<sup>3</sup>/sec was not consistent with the trends probably due to the missed trailing edge at Kalamazoo for which the concentrations were extrapolated. Therefore, a dispersion value of 8.51 m<sup>2</sup>/sec was calculated by interpolating the dispersion values at 14.41 m<sup>3</sup>/sec and 19.06 m<sup>3</sup>/sec. Also,

as the sampling for  $2.06 \text{ m}^3/\text{sec}$  was only done at Farm Lane Br and Kalamazoo Bridge, and the data real time concentration data were not available at Kellogg Bridge, a dispersion coefficient value of  $5.20 \text{ m}^2/\text{sec}$  was determined by interpolating the values for Farm lane and Kalamazoo Bridge.

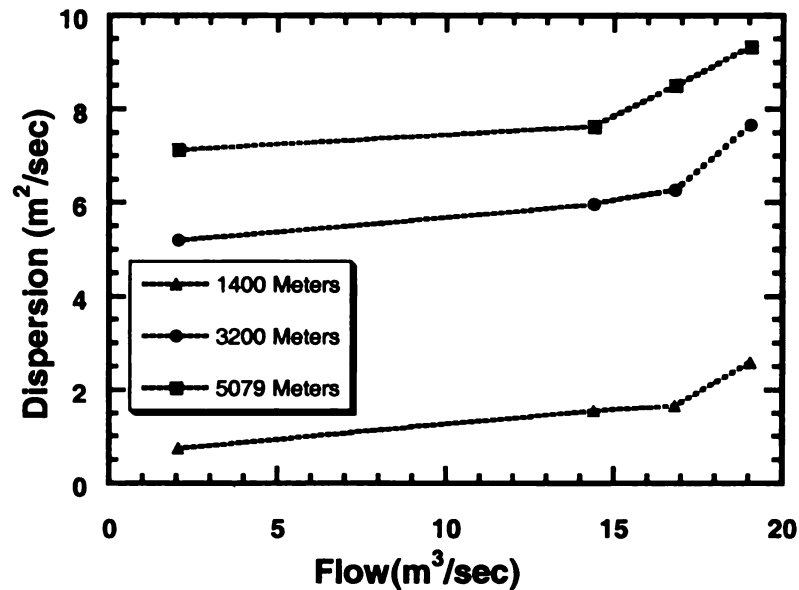


Figure 5-26. Dispersion coefficient calculated using mass transport equation under different flow conditions.

The dispersion coefficient increased with distance also, as the water column moved downstream, however the rate of increase in dispersion decreased as the dye cloud moved further downstream. The change in dispersion with distance at different flow conditions can be observed in (Figure 5-27).

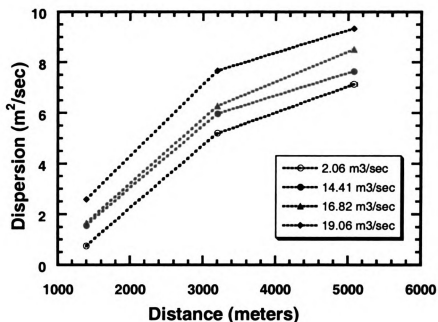


Figure 5-27. Dispersion coefficient at different downstream sampling locations.

The application of one-dimensional advection-dispersion equation is limited to zones of complete mixing as reported in the literature therefore it is essential that the zone of complete mixing be determined in order to justify its application. The mixing length in this case was determined to lie between 2,800 meters to 3,200 meters for a medium flow range using the formula by Fischer (1979) for centerline injection. In real practice the tracer was not dumped in the center but was poured instantaneously at the middle 75% of the width so that a quasi-instantaneous mixing is achieved, therefore the mixing length is not assumed to extend to calculated 2,800 meters length. Also, the sinuous nature of the river meanders in the initial 1000 meters also enhances the process of mixing. But on the other hand, the samples at different point at Bogue Street Bridge located at 850 meters from the injection point indicate a variation of 27.37 % in peak concentrations and 12.7

% in areas under the curve (Table 5-10); which indicate a non-homogeneous domain. Due to positive slope between Bogue Bridge and the Farm Lane Bridge, and the effect of the damming action of the weir, the mixing length is assumed to extend beyond Farm Lane Bridge up to the weir. Beyond weir, the channel could safely be assumed as completely mixed. At low flow, the lack of turbulence increases the time for transverse mixing. However, at medium flow and high flow, the turbulence and formation of whirl pools and eddies can physically be observed, so transverse mixing time is reduced considerably.

Table 5-10. Variation in concentration across a transect indicating the state of lateral mixing.

Location	Area Under Time-Concentration. Curve	Percent Variation From Centre	Peak Concentration.	Percent Variation From Centre
Left	2284.3	-12.7	52	-27.37
Centre	2618.1	-	71.6	-
Right	2761.68	+ 5.48	65	-9.2

Although settling, entrainment and transformation affect the peak concentrations exponentially; the effect of the dye loss was not taken into account because the dye recovery calculated could not be justified. In all the cases, the dye recovery was a little more than the amount actually dumped. This was however attributed to the conditions of incomplete mixing specially under the low flow conditions.

The classical application of the analytical solution of 1-D advection dispersion equation, when used with a constant value of dispersion coefficient, is based on the assumption of a channel of uniform cross section for entire length in order to predict the concentrations at a downstream location. If a constant value of dispersion coefficient is used, there is a decrease in the peak concentrations and increase in the spread as a contaminant travels downstream, but the area under the time-concentration curve remains the same. In this case the width varies between 16 meters to 40 meters and so does the cross sectional area, therefore the channel is characterized as non-uniform. The dispersion coefficients were calculated for each sampling point basing on the observed peak concentrations and the time for peak concentration. These values of dispersion coefficients were used to predict the passage of the dye cloud through all the three sampling points and respective areas under each time-concentration curve were calculated. By use of different values, although the areas under each concentration curve should remain the same, the overall shape of the time-concentration curve should coincide with the observed time-concentration curve. The area under the time-concentration curve for calculated concentrations (Table 5-11) shows a variation of 3.9 %, which is due to a variation in flow over the sampling period. However, the area under the curve for observed concentration shows a variation of 14.8 %, 12.2 % and 16.07 % for 14.41 m<sup>3</sup>/sec, 16.82 m<sup>3</sup>/sec and 16.82 m<sup>3</sup>/sec flow between the three sampling locations (Table 5-12). These areas were found to be 17 % to 46 % more as compared to those calculated by analytical solution for one dimensional advection-dispersion equation (Table 5-13), which indicates that the equation does not take into account the effects of storage zone presumed to be responsible for the prolonged evolution of the trailing edge

of the dye cloud. Nevertheless, this equation still can serve a good purpose in quantification of longitudinal dispersion as the dispersion coefficients calculated by this equation can make a good match of the rising limb and the peak concentrations.

Table 5-11. Area under time-concentration curves for calculated concentration.

Flow	Area Under Time Concentration Curves		
	Farm Lane Bridge	Kellogg Bridge	Kalamazoo Bridge
14.41 m <sup>3</sup> /sec	1035.50	1053.19	1065.00
16.82 m <sup>3</sup> /sec	470.17	462.45	472.53
19.06 m <sup>3</sup> /sec	935.00	951.00	973.00

Note: The area under the time-concentration curves has been calculated by using the analytical solution for one-dimensional advection-dispersion coefficient with different values of dispersion coefficient

Table 5-12. Area under time-concentration curves for observed concentrations.

Flow	Area Under Time Concentration Curves		
	Farm Lane Bridge	Kellogg Bridge	Kalamazoo Bridge
14.41 m <sup>3</sup> /sec	1393.46	1243.48	1459.37
16.82 m <sup>3</sup> /sec	630.885	596.00	553.70
19.06 m <sup>3</sup> /sec	1195.00	1275.85	1423.95

Table 5-13. Comparison of areas under the time-concentration curve for predicted and observed concentrations.

Flow	Net % Increase in Area Under Time Concentration Curve		
	Farm Lane Bridge	Kellogg Bridge	Kalamazoo Bridge
14.41 m <sup>3</sup> /sec	34.57	18.07	37.03
16.82 m <sup>3</sup> /sec	34.18	28.88	17.18
19.06 m <sup>3</sup> /sec	27.81	34.16	46.35

Note: The figures indicate percent increase in area under the time concentration curves for the observed concentrations compared with the concentrations calculated using one-dimensional advection dispersion equation.

As the one-dimensional advection-dispersion equation is limited to the zones of complete mixing, the calculated dispersion coefficients increase sharply with distance between first and the second sampling point. However, the increase in dispersion becomes less in magnitude as the dye cloud moves further downstream. In a well-mixed

zone, the dye cloud evolution should approach a gaussian shape by use of a constant value of dispersion coefficient. Although the dispersion coefficients calculated for the second and third sampling point tend to increase with distance, the increase is much less as compared to the increase between first and second sampling station, so the use of a constant value of dispersion coefficient in the reach beyond the Farm Lane Bridge did not alter much the time-concentration profiles.

In this case, the little increase in dispersion coefficient in the well-mixed zone can be attributed to the change in width of the river across the river reach. The change in the width along the reach effects the longitudinal dispersion due to sharpness or flatness of the transverse velocity profile. These different values of dispersion coefficients calculated for each sampling location were plugged in equation (5-6) to predict the concentrations at the three sampling points for all five-dye releases. The relationships between observed and predicted concentrations using equation (5-6) are presented in (Figure 5-28) through (Figure 5-28). The predicted concentrations in these figures correspond to the analytical solution for one-dimensional advection-dispersion equation.



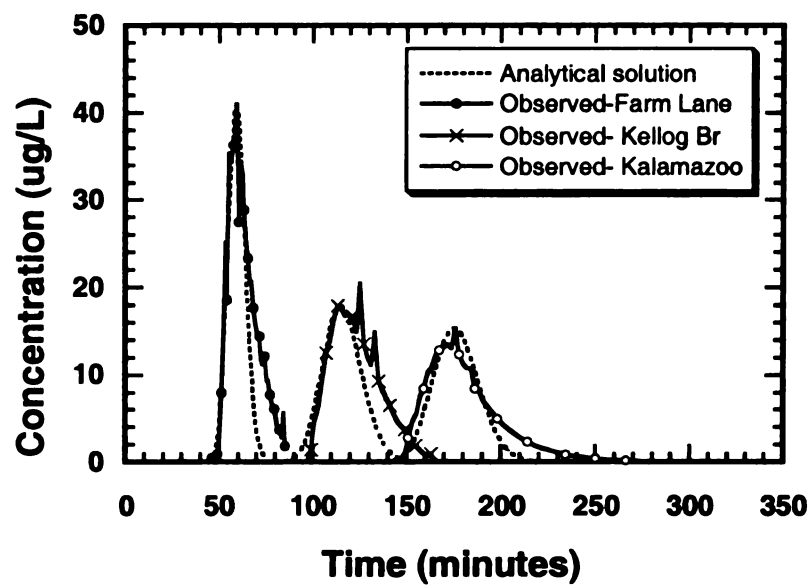


Figure 5-28. Predicted and observed concentration at 16.82 m<sup>3</sup>/sec flow.

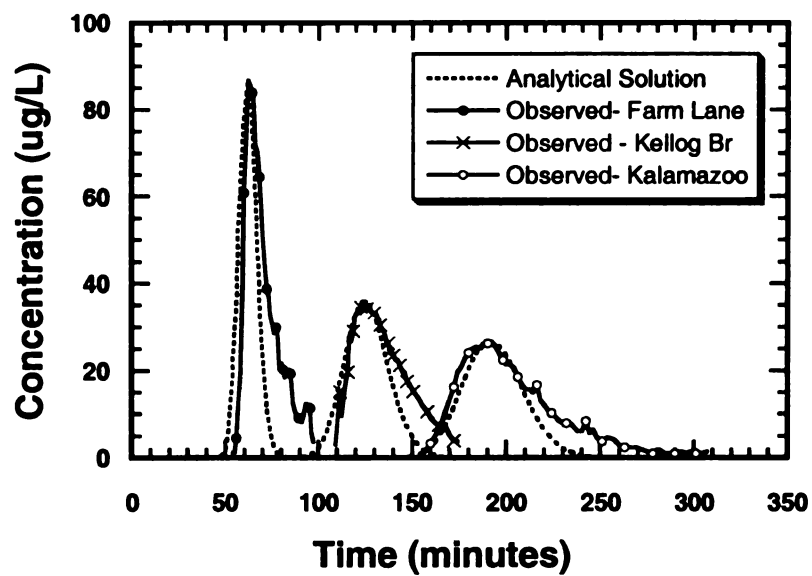


Figure 5-29. Predicted and observed concentration at 14.41 m<sup>3</sup>/sec flow.

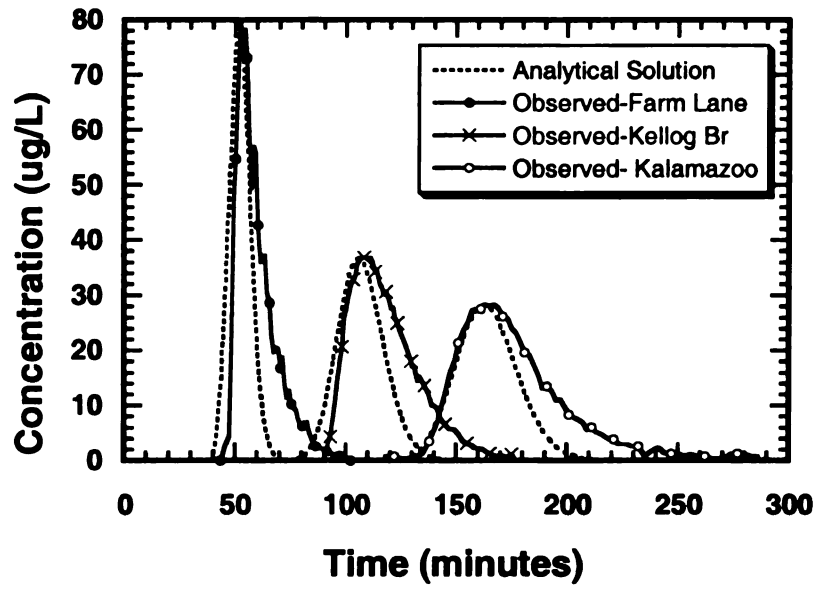


Figure 5-30. Predicted and observed concentration at  $19.3 \text{ m}^3/\text{sec}$  flow.

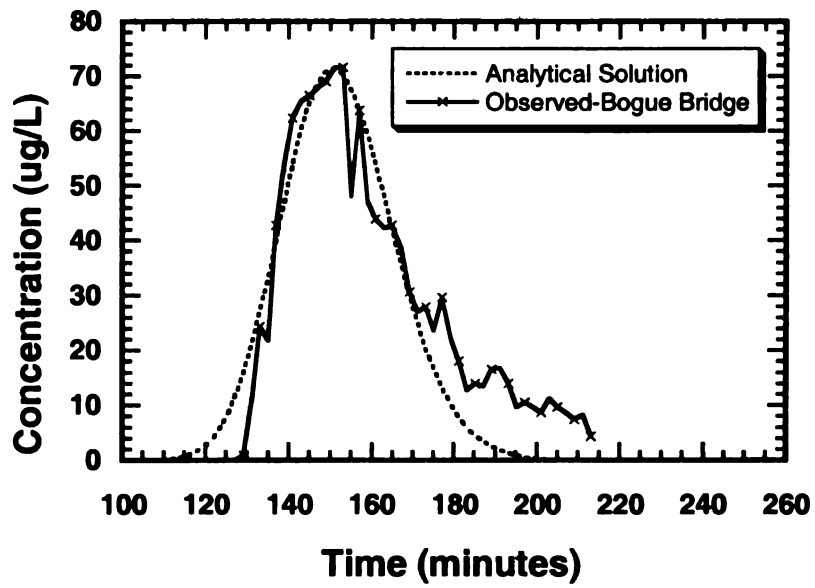


Figure 5-31. Predicted and observed concentration at  $2.49 \text{ m}^3/\text{sec}$  flow.

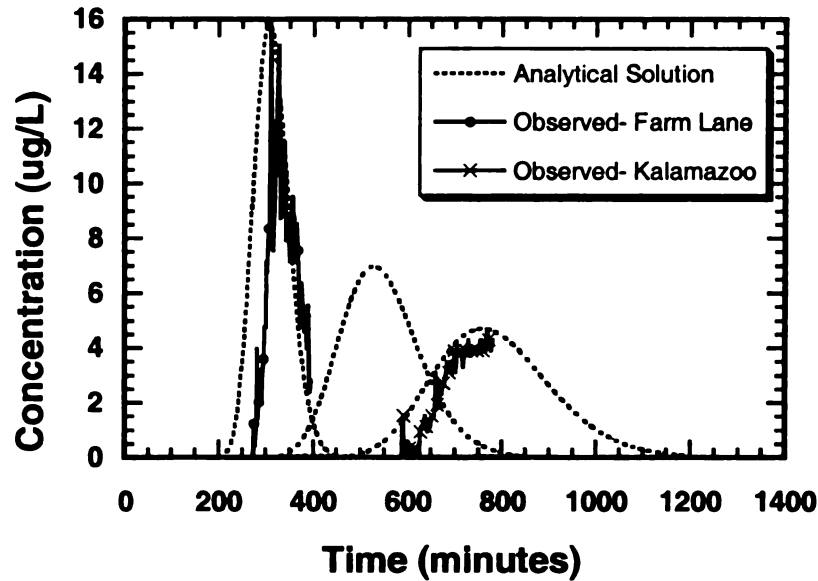


Figure 5-32 Predicted and observed concentration at 2.06 m<sup>3</sup>/sec flow.

In order to plot a concentration profile at any point downstream the value of dispersion coefficient must be known. The observed data yielded two different sets of linear equations. The first set of equations comprises dispersion as a function of distance from the injection point at a given flow condition. The second set of equations gave dispersion as a function of flow at different points down stream. The statistical combination of two different sets of equation yielded a single equation for dispersion with two variables i.e. distance and flow.

$$D_x = 0.104Q + 0.001767x - 1.713 \quad (5-8)$$

Where:

$Q$  = Flow (m<sup>3</sup>/sec)

$x$  = Distance downstream from the injection point (m)

The values of dispersion coefficient were recalculated using equation (5-8) and are presented in (Table 5-14).

Table 5-14. Comparison of calculated and predicted dispersion coefficients.

Flow (m <sup>3</sup> /sec)	Dispersion Coefficient (m <sup>2</sup> /sec)					
	Distance from injection point (m)					
	1400		3200		5079	
	Calc by Analytical Solution	Predicted by Empirical Equation	Calc by Analytical Solution	Predicted by Empirical Equation	Calc by Analytical Solution	Predicted by Empirical Equation
2.06	0.74	0.97	5.2	4.25	7.13	7.47
14.41	1.55	2.25	5.96	5.44	7.63	8.76
16.82	1.65	2.51	6.27	5.69	8.51	9.01
19.06	2.58	2.74	7.66	5.92	9.33	9.24

An x-y plot of these two set of dispersion coefficients yields a linear relationship with a correlation coefficient of 0.95985 (Figure 5-33)

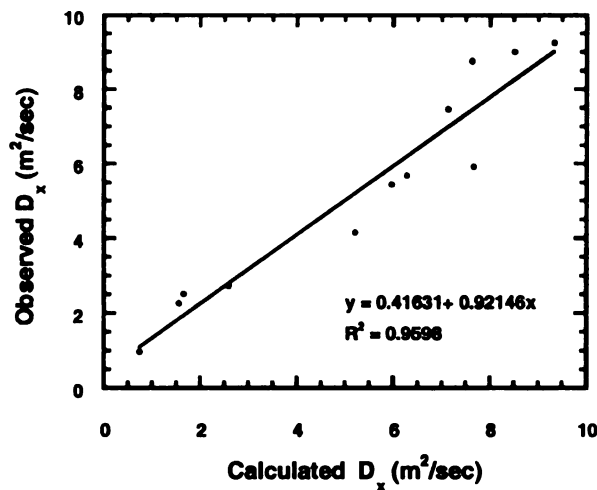


Figure 5-33. Relation between calculated and predicted dispersion coefficients.

A relation for prediction of the peak concentration time at any point downstream based on the dye study data could only be established for the medium flow condition. The following correlation is:

$$T_p = 0.3826Q + 0.0338x \quad (5-9)$$

where:

$T_p$  = time for peak concentration (minutes)

$Q$  = discharge ( $\text{m}^3/\text{sec}$ )

$x$  = distance downstream from injection (meters)

The values of the peak arrival time recalculated using this equation exhibit good correlation with the observed values, with an  $R^2$  value of 0.96 however, it does not hold good for the low flow condition.

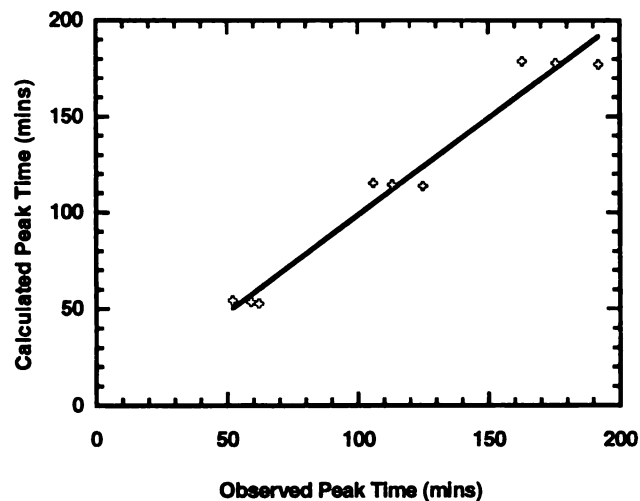


Figure 5-34. Calculated and observed peak arrival time.

The equations for peak time ( $T_p$ ) and dispersion coefficient ( $Dx$ ) can be used in predicting the downstream concentrations at any point while knowing only the discharge which is available at the USGS Gage at half hour intervals. Of course, the validity of these equations is, only for medium flow conditions. Another limitation is that these values are to be used into the analytical solution for conventional 1-D advection – dispersion equation that is applicable only to the well-mixed conditions and it doesn't take into account the dead zones, more commonly described as “storage zones” in the current literature therefore, the skewed nature of the time-concentration curve cannot be predicted. The summary of the empirical equations to predict the concentration of a conservative contaminant is as follows with known discharge in m<sup>3</sup>/sec and known mass in grams.

$$T_p = 0.3826Q + 0.0338x$$

$$Dx = 0.104Q + 0.001767x - 1.713$$

$$u = x/T_p$$

$$A = Q/u$$

$$C(x,t) = \left[ \frac{M}{2A\sqrt{\pi Dx t}} \right] \exp \left[ \frac{-(x - ut)^2}{4Dxt} \right]$$

This procedure was applied to predict the time concentration curves for the tracer tests. The predicted and observed concentrations are presented in the following figures. However, a lag in time was observed for the Farm Lane Bridge, for which the actual velocity is less than the predicted velocity due to an upward slope in the portion between the Hagadorn Bridge and the Farm Lane Bridge, therefore a factor of 1.1 was used to

predict the peak time ( $T_p$ ) with empirical equation. This factor was not used for a flow of  $19.06 \text{ m}^3/\text{sec}$ .

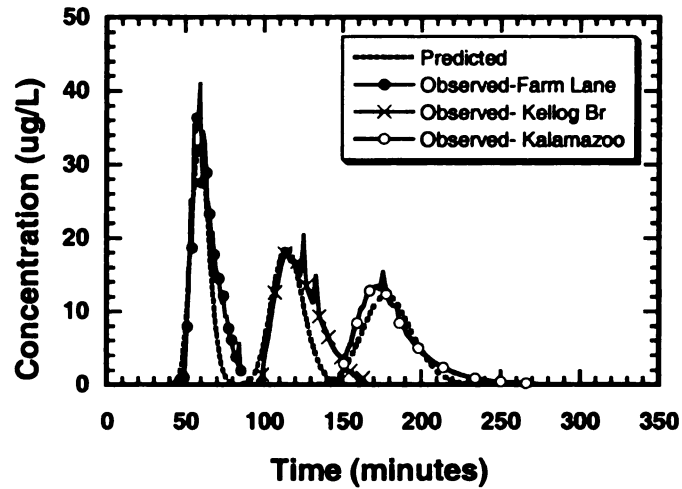


Figure 5-35. Predicted and observed concentration using empirical relations at  $16.82 \text{ m}^3/\text{sec}$  flow.

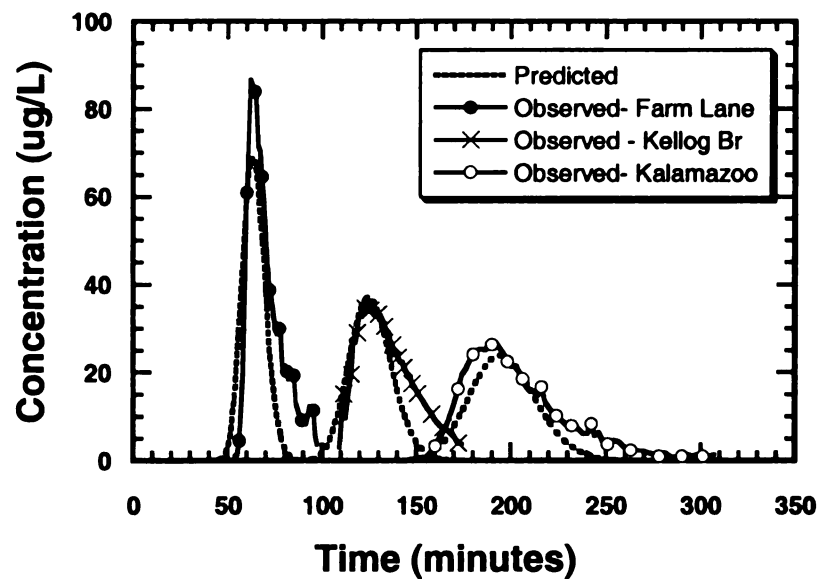


Figure 5-36. Predicted and observed concentration using empirical relations at  $14.41 \text{ m}^3/\text{sec}$  flow.

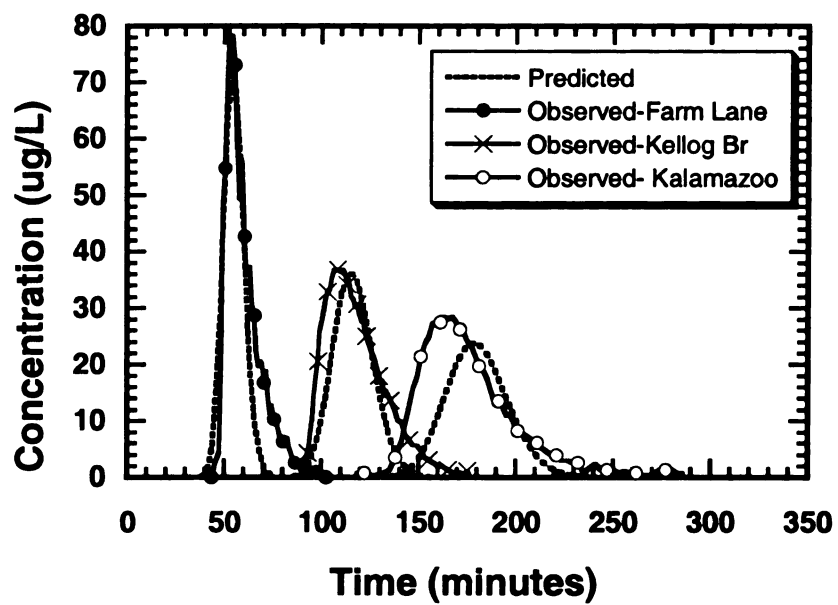


Figure 5-37 Predicted and observed concentration using empirical relations at 19.06 m<sup>3</sup>/sec flow



## 6. CONCLUSIONS

The velocities and heads predicted by the one-dimensional model for Red Cedar River based on DYNHYD are in reasonable agreement with the field measurements. Further model refinement may be required to improve predictions at the Kellogg Bridge where the model could not capture the variability in hydrodynamics due to sharp bends. The model predicted results are more reliable for use in any contaminant transport model over the reach average values. The river reach exhibited dispersion characteristics, which varied with distance and the flow condition. The increase in the dispersion coefficient with distance was found to be more pronounced in the initial reach extending a little beyond the Farm Lane Bridge up to weir, which falls within the initial mixing length, therefore the sub reach of the river bounded by Hagadorn road and MSU library bridge could not be characterized with a constant value of dispersion coefficient. However, the rate of increase in dispersion coefficient beyond the initial reach sharply reduces tending to reach a constant value. This less increase in the dispersion coefficient with distance as compared with the initial sub reach is viewed to be a result of the variation in width of the river, which narrows as it approaches the lower bounds, giving rise to a higher transverse velocity profile, which increases dispersion longitudinally. The empirical equation developed allow the calculation of dispersion coefficient at any point of the MSU river reach for a particular flow condition by with a reasonable accuracy, but is site specific in

nature because as the basis of these equations are site specific tracer tests and hence cannot be applied beyond the reach or to any other site.

## 7. APPENDICES

### Appendix A Junction and Channel Properties

Junction Number	Channel Number	Width (m)	Junction Surface Area (m <sup>2</sup> )	Bottom Elevation (m)	Angle (Degrees)
1			699.5	0	
2	1	28.0	1352.6	0.0000	70
3	2	26.1	1378.5	0.0036	70
4	3	29.0	1626.1	0.0072	74
5	4	36.0	1772.4	0.0108	68
6	5	34.9	1652.8	0.0143	63
7	6	31.2	1588.0	0.0179	68
8	7	32.3	1715.3	0.0215	71
9	8	36.3	1645.2	0.0251	90
10	9	29.5	1407.4	0.0287	105
11	10	26.8	1521.7	0.0323	120
12	11	34.0	1685.5	0.0359	134
13	12	33.4	1815.1	0.0394	131
14	13	39.2	1902.1	0.0430	119
15	14	36.9	1624.7	0.0466	106
16	15	28.1	1393.6	0.0502	92
17	16	27.6	1518.7	0.0538	87
18	17	33.1	1690.1	0.0574	95
19	18	34.5	1758.7	0.0610	101
20	19	35.9	1765.6	0.0991	105
21	20	34.7	1820.4	0.1372	109
22	21	38.1	1830.3	0.1753	104
23	22	35.1	1739.6	0.2134	106
24	23	34.4	1671.8	0.2515	102
25	24	32.4	1584.2	0.2896	102
26	25	30.9	1495.0	0.3277	94
27	26	28.9	1540.8	0.3658	84
28	27	32.8	1601.7	0.4039	80
29	28	31.3	1536.2	0.4420	80

Junction and Channel Properties...continued

<b>Junction Number</b>	<b>Channel Number</b>	<b>Width (m)</b>	<b>Junction Surface Area (m<sup>2</sup>)</b>	<b>Bottom Elevation (m)</b>	<b>Angle (Degrees)</b>
30	29	30.1	1401.7	0.3644	71
31	30	25.9	1341.5	0.2868	66
32	31	27.7	1488.9	0.2092	64
33	32	31.8	1514.6	0.1316	64
34	33	28.8	1385.8	0.0540	64
35	34	26.7	1387.8	-0.0236	51
36	35	28.8	1340.1	-0.1011	56
37	36	24.8	1279.2	-0.1787	53
38	37	26.4	1373.4	-0.2563	59
39	38	28.5	1449.1	-0.3339	63
40	39	29.4	1427.1	-0.4115	60
41	40	27.6	1385.3	-0.4158	60
42	41	27.8	1260.3	-0.4202	50
43	42	22.6	1152.9	-0.4245	48
44	43	23.5	1252.0	-0.4289	51
45	44	26.6	1339.1	-0.4333	50
46	45	27.0	1259.4	-0.4376	46
47	46	23.4	1022.0	-0.4420	34
48	47	17.5	844.9	-0.4689	8
49	48	16.3	913.6	-0.4957	7
50	49	20.2	974.2	-0.5226	59
51	50	18.8	962.0	-0.5495	64
52	51	19.7	1045.5	-0.5764	74
53	52	22.1	1106.4	-0.6033	88
54	53	22.2	1342.6	-0.6302	95
55	54	31.5	1559.8	-0.6571	101
56	55	30.8	1539.2	-0.6840	90
57	56	30.7	1501.1	-0.7109	105
58	57	29.3	1449.3	-0.7378	100
59	58	28.7	1259.1	-0.7647	147
60	59	21.7	1030.1	-0.7916	204
61	60	19.5	1039.1	-0.8185	216
62	61	22.1	1190.0	-0.8454	209
63	62	25.5	1298.8	-0.8723	203

Junction and Channel Properties...continued

<b>Junction Number</b>	<b>Channel Number</b>	<b>Width (m)</b>	<b>Junction Surface Area (m<sup>2</sup>)</b>	<b>Bottom Elevation (m)</b>	<b>Angle (Degrees)</b>
64	63	26.4	1417.3	-0.8992	197
65	64	30.3	1457.2	-0.9627	176
66	65	28.0	1307.0	-1.0262	151
67	66	24.3	1148.7	-1.0897	108
68	67	21.7	1107.1	-1.1532	96
69	68	22.6	1267.3	-1.2167	101
70	69	28.1	1293.6	-1.2802	101
71	70	23.7	1237.3	-1.3088	94
72	71	25.8	1371.3	-1.3375	87
73	72	29.0	1383.5	-1.3662	92
74	73	26.3	1294.3	-1.3949	95
75	74	25.4	1473.2	-1.4236	82
76	75	33.5	1516.8	-1.4523	65
77	76	27.2	1334.5	-1.4810	80
78	77	26.2	1367.6	-1.5097	106
79	78	28.5	1381.0	-1.5383	107
80	79	26.7	1274.7	-1.5670	130
81	80	24.3	1454.4	-1.5957	168
82	81	33.9	1527.3	-1.6244	120
83	82	27.2	1290.7	-1.6531	100
84	83	24.5	1238.7	-1.6818	74
85	84	25.1	1240.7	-1.7105	67
86	85	24.5	1391.2	-1.7392	22
87	86	31.1	1687.4	-1.7678	6
88	87	36.4	1452.9	-1.7965	86
89	88	21.7	1287.6	-1.8252	143
90	89	29.8	1754.2	-1.8539	127
91	90	40.4	2017.5	-1.8826	61
92	91	40.3	1927.3	-1.9113	21
93	92	36.8	1640.8	-1.9400	102
94	93	28.8	1418.7	-1.9686	179
95	94	27.9	1304.5	-1.9973	165
96	95	24.3	1455.4	-2.0260	150
97	96	33.9	1316.1	-2.0547	136

Junction and Channel Properties...continued

<b>Junction Number</b>	<b>Channel Number</b>	<b>Width (m)</b>	<b>Junction Surface Area (m<sup>2</sup>)</b>	<b>Bottom Elevation (m)</b>	<b>Angle (Degrees)</b>
98	97	18.7	954.1	-2.0834	134
99	98	19.5	965.0	-2.1121	122
100	99	19.1	990.5	-2.1408	134
101	100	20.5	1091.2	-2.1695	134
102	101	23.2	1142.5	-2.1981	136
103	102	22.5	563.6	-2.2268	136

## Appendix B Input File

MODELING OF RED CEDAR RIVER  
MICH STATE UNIV, EAST LANSING.

\*\*\*\*\* PROGRAM CONTROL DATA \*\*\*\*\*

103 102 0 5 5 1 0300 8 2330

\*\*\*\*\* OUTPUT CONTROL DATA \*\*\*\*\*

0.0000E-01 0.500 103

1	2	3	4	5	6	7	8	9	10	11	12	13	14	15	16
17	18	19	20	21	22	23	24	25	26	27	28	29	30	31	32
33	34	35	36	37	38	39	40	41	42	43	44	45	46	47	48
49	50	51	52	53	54	55	56	57	58	59	60	61	62	63	64
65	66	67	68	69	70	71	72	73	74	75	76	77	78	79	80
81	82	83	84	85	86	87	88	89	90	91	92	93	94	95	96
97	98	99	100	101	102	103									

\*\*\*\*\* HYDRAULIC SUMMARY CONTROL DATA \*\*\*\*\*

1 1 63012.50 1 1

\*\*\*\*\* JUNCTION DATA \*\*\*\*\*

1	2.0	699.5	0.0	1	0	0	0	0	0
2	2.0	1352.6	0.0	1	2	0	0	0	0
3	2.0	1378.5	.0036	2	3	0	0	0	0
4	2.0	1626.1	.0072	3	4	0	0	0	0
5	2.0	1772.4	.0108	4	5	0	0	0	0
6	2.0	1652.8	.0143	5	6	0	0	0	0
7	2.0	1588.0	.0179	6	7	0	0	0	0
8	2.0	1715.3	.0215	7	8	0	0	0	0
9	2.0	1645.2	.0251	8	9	0	0	0	0
10	2.0	1407.4	.0287	9	10	0	0	0	0
11	2.0	1521.7	.0323	10	11	0	0	0	0
12	2.0	1685.5	.0359	11	12	0	0	0	0
13	2.0	1815.1	.0394	12	13	0	0	0	0
14	2.0	1902.1	.0430	13	14	0	0	0	0
15	2.0	1624.7	.0466	14	15	0	0	0	0
16	2.0	1393.6	.0502	15	16	0	0	0	0
17	2.0	1518.7	.0538	16	17	0	0	0	0
18	2.0	1690.1	.0574	17	18	0	0	0	0
19	2.0	1758.7	.0610	18	19	0	0	0	0
20	2.0	1765.6	.0991	19	20	0	0	0	0
21	2.0	1820.4	.1372	20	21	0	0	0	0
22	2.0	1830.3	.1753	21	22	0	0	0	0
23	2.0	1739.6	.2134	22	23	0	0	0	0

Input File.... Continued

24	2.0	1671.8	.2515	23	24	0	0	0	0
25	2.0	1584.2	.2896	24	25	0	0	0	0
26	2.0	1495.0	.3277	25	26	0	0	0	0
27	2.0	1540.8	.3658	26	27	0	0	0	0
28	2.0	1601.7	.4039	27	28	0	0	0	0
29	2.0	1536.2	.4420	28	29	0	0	0	0
30	2.0	1401.7	.3644	29	30	0	0	0	0
31	2.0	1341.5	.2868	30	31	0	0	0	0
32	2.0	1488.9	.2092	31	32	0	0	0	0
33	2.0	1514.6	.1316	32	33	0	0	0	0
34	2.0	1385.8	.0540	33	34	0	0	0	0
35	2.0	1387.8	-.0236	34	35	0	0	0	0
36	2.0	1340.1	-.1011	35	36	0	0	0	0
37	2.0	1259.1	-.1787	36	37	0	0	0	0
38	2.0	1080.3	-.2563	37	38	0	0	0	0
39	2.0	1449.1	-.3339	38	39	0	0	0	0
40	2.0	1427.1	-.4115	39	40	0	0	0	0
41	2.0	1385.3	-.4158	40	41	0	0	0	0
42	2.0	1260.3	-.4202	41	42	0	0	0	0
43	2.0	1152.9	-.4245	42	43	0	0	0	0
44	2.0	1252.0	-.4289	43	44	0	0	0	0
45	2.0	1339.1	-.4333	44	45	0	0	0	0
46	2.0	1259.4	-.4376	45	46	0	0	0	0
47	2.0	1022.0	-.4420	46	47	0	0	0	0
48	2.0	844.9	-.4689	47	48	0	0	0	0
49	2.0	913.6	-.4957	48	49	0	0	0	0
50	2.0	974.2	-.5226	49	50	0	0	0	0
51	2.0	962.0	-.5495	50	51	0	0	0	0
52	2.0	1045.5	-.5764	51	52	0	0	0	0
53	2.0	1106.4	-.6033	52	53	0	0	0	0
54	2.0	1342.6	-.6302	53	54	0	0	0	0
55	2.0	1559.8	-.6571	54	55	0	0	0	0
56	2.0	1539.2	-.6840	55	56	0	0	0	0
57	2.0	1501.1	-.7109	56	57	0	0	0	0
58	2.0	1449.3	-.7378	57	58	0	0	0	0
59	2.0	1259.1	-.7647	58	59	0	0	0	0
60	2.0	1080.3	-.7916	59	60	0	0	0	0
61	2.0	1140.0	-.8185	60	61	0	0	0	0
62	2.0	1265.0	-.8454	61	62	0	0	0	0

Input File.... Continued



63	2.0	1323.0	-.8723	62	63	0	0	0	0
64	2.0	1417.3	-.8992	63	64	0	0	0	0
65	2.0	1457.2	-.9627	64	65	0	0	0	0
66	2.0	1307.0	-1.0262	65	66	0	0	0	0
67	2.0	1148.7	-1.0897	66	67	0	0	0	0
68	2.0	1107.1	-1.1532	67	68	0	0	0	0
69	2.0	1267.3	-1.2167	68	69	0	0	0	0
70	2.0	1293.6	-1.2802	69	70	0	0	0	0
71	2.0	1237.3	-1.3088	70	71	0	0	0	0
72	2.0	1371.3	-1.3375	71	72	0	0	0	0
73	2.0	1383.5	-1.3662	72	73	0	0	0	0
74	2.0	1294.3	-1.3949	73	74	0	0	0	0
75	2.0	1473.2	-1.4236	74	75	0	0	0	0
76	2.0	1516.8	-1.4523	75	76	0	0	0	0
77	2.0	1334.5	-1.4810	76	77	0	0	0	0
78	2.0	1367.6	-1.5097	77	78	0	0	0	0
79	2.0	1381.0	-1.5383	78	79	0	0	0	0
80	2.0	1274.7	-1.5670	79	80	0	0	0	0
81	2.0	1454.4	-1.5957	80	81	0	0	0	0
82	2.0	1527.3	-1.6244	81	82	0	0	0	0
83	2.0	1290.7	-1.6531	82	83	0	0	0	0
84	2.0	1238.7	-1.6818	83	84	0	0	0	0
85	2.0	1240.7	-1.7105	84	85	0	0	0	0
86	2.0	1391.2	-1.7392	85	86	0	0	0	0
87	2.0	1687.4	-1.7678	86	87	0	0	0	0
88	2.0	1452.9	-1.7965	87	88	0	0	0	0
89	2.0	1287.6	-1.8252	88	89	0	0	0	0
90	2.0	1754.2	-1.8539	89	90	0	0	0	0
91	2.0	2017.5	-1.8826	90	91	0	0	0	0
92	2.0	1927.3	-1.9113	91	92	0	0	0	0
93	2.0	1640.8	-1.9400	92	93	0	0	0	0
94	2.0	1418.7	-1.9686	93	94	0	0	0	0
95	2.0	1304.5	-1.9973	94	95	0	0	0	0
96	2.0	1455.4	-2.0260	95	96	0	0	0	0
97	2.0	1316.1	-2.0547	96	97	0	0	0	0
98	2.0	954.1	-2.0834	97	98	0	0	0	0
99	2.0	965.0	-2.1121	98	99	0	0	0	0
100	2.0	990.5	-2.1408	99	100	0	0	0	0
101	2.0	1091.2	-2.1695	100	101	0	0	0	0
102	2.0	1142.5	-2.1981	101	102	0	0	0	0
103	2.0	563.6	-2.2268	102	103	0	0	0	0

\*\*\*\*\* CHANNEL DATA \*\*\*\*\*

1	50	28.0	0.0	70	0.0210	0.00	1	2
---	----	------	-----	----	--------	------	---	---

Input File.... Continued

2	50	26.1	0.0	74	0.0210	0.00	2	3
3	50	29.0	0.0	74	0.0210	0.00	3	4
4	50	36.0	0.0	68	0.0210	0.00	4	5
5	50	34.9	0.0	63	0.0210	0.00	5	6
6	50	31.2	0.0	68	0.0210	0.00	6	7
7	50	32.3	0.0	71	0.0210	0.00	7	8
8	50	36.3	0.0	90	0.0210	0.00	8	9
9	50	29.5	0.0	105	0.0210	0.00	9	10
10	50	26.8	0.0	120	0.0210	0.00	10	11
11	50	34.0	0.0	134	0.0210	0.00	11	12
12	50	33.4	0.0	131	0.0210	0.00	12	13
13	50	39.2	0.0	119	0.0210	0.00	13	14
14	50	36.9	0.0	106	0.0210	0.00	14	15
15	50	28.1	0.0	92	0.0210	0.00	15	16
16	50	27.6	0.0	87	0.0210	0.00	16	17
17	50	33.1	0.0	95	0.0210	0.00	17	18
18	50	34.5	0.0	101	0.0320	0.00	18	19
19	50	35.9	0.0	105	0.0320	0.00	19	20
20	50	34.7	0.0	109	0.0320	0.00	20	21
21	50	38.1	0.0	104	0.0320	0.00	21	22
22	50	35.1	0.0	106	0.0320	0.00	22	23
23	50	34.4	0.0	102	0.0320	0.00	23	24
24	50	32.4	0.0	102	0.0320	0.00	24	25
25	50	30.9	0.0	94	0.0320	0.00	25	26
26	50	28.9	0.0	84	0.0320	0.00	26	27
27	50	32.8	0.0	80	0.0320	0.00	27	28
28	50	31.3	0.0	80	0.0360	0.00	28	29
29	50	30.1	0.0	71	0.0360	0.00	29	30
30	50	25.9	0.0	66	0.0360	0.00	30	31
31	50	27.7	0.0	64	0.0360	0.00	31	32
32	50	31.8	0.0	64	0.0360	0.00	32	33
33	50	28.8	0.0	64	0.0360	0.00	33	34
34	50	26.7	0.0	51	0.0360	0.00	34	35
35	50	28.8	0.0	56	0.0360	0.00	35	36
36	50	24.8	0.0	53	0.0360	0.00	36	37
37	50	26.4	0.0	59	0.0360	0.00	37	38
38	50	26.5	0.0	63	0.0360	0.00	38	39
39	50	29.4	0.0	60	0.0220	0.00	39	40
40	50	27.6	0.0	60	0.0220	0.00	40	41
41	50	27.8	0.0	50	0.0220	0.00	41	42
42	50	22.6	0.0	48	0.0220	0.00	42	43
43	50	23.5	0.0	51	0.0220	0.00	43	44
44	50	26.6	0.0	50	0.0220	0.00	44	45

Input File.... Continued

45	50	27.0	0.0	46	0.0220	0.00	45	46
46	50	23.4	0.0	34	0.0310	0.00	46	47
47	50	17.5	0.0	8	0.0310	0.00	47	48
48	50	16.3	0.0	7	0.0310	0.00	48	49
49	50	20.2	0.0	59	0.0310	0.00	49	50
50	50	18.8	0.0	64	0.0310	0.00	50	51
51	50	19.7	0.0	74	0.0310	0.00	51	52
52	50	22.1	0.0	88	0.0310	0.00	52	53
53	50	22.2	0.0	95	0.0310	0.00	53	54
54	50	31.5	0.0	101	0.0310	0.00	54	55
55	50	30.8	0.0	90	0.0310	0.00	55	56
56	50	30.7	0.0	105	0.0310	0.00	56	57
57	50	29.3	0.0	100	0.0310	0.00	57	58
58	50	28.7	0.0	147	0.0310	0.00	58	59
59	50	21.7	0.0	204	0.0310	0.00	59	60
60	50	21.5	0.0	216	0.0310	0.00	60	61
61	50	24.1	0.0	209	0.0310	0.00	61	62
62	50	26.5	0.0	203	0.0310	0.00	62	63
63	50	26.4	0.0	197	0.0360	0.00	63	64
64	50	30.3	0.0	176	0.0360	0.00	64	65
65	50	28.0	0.0	151	0.0360	0.00	65	66
66	50	24.3	0.0	108	0.0360	0.00	66	67
67	50	21.7	0.0	96	0.0360	0.00	67	68
68	50	22.6	0.0	101	0.0360	0.00	68	69
69	50	28.1	0.0	101	0.0310	0.00	69	70
70	50	23.7	0.0	94	0.0310	0.00	70	71
71	50	25.8	0.0	87	0.0310	0.00	71	72
72	50	29.0	0.0	92	0.0310	0.00	72	73
73	50	26.3	0.0	95	0.0310	0.00	73	74
74	50	25.4	0.0	82	0.0310	0.00	74	75
75	50	33.5	0.0	65	0.0310	0.00	75	76
76	50	27.2	0.0	80	0.0310	0.00	76	77
77	50	26.2	0.0	106	0.0310	0.00	77	78
78	50	28.5	0.0	107	0.0310	0.00	78	79
79	50	26.7	0.0	130	0.0310	0.00	79	80
80	50	24.3	0.0	168	0.0310	0.00	80	81
81	50	33.9	0.0	120	0.0310	0.00	81	82
82	50	27.2	0.0	100	0.0310	0.00	82	83
83	50	24.5	0.0	74	0.0310	0.00	83	84
84	50	25.1	0.0	67	0.0310	0.00	84	85
85	50	24.5	0.0	22	0.0310	0.00	85	86
86	50	31.1	0.0	6	0.0310	0.00	86	87
87	50	36.4	0.0	86	0.0310	0.00	87	88

Input File.... Continued

88	50	21.7	0.0	143	0.0310	0.00	88	89
89	50	29.8	0.0	127	0.0310	0.00	89	90
90	50	40.4	0.0	61	0.0310	0.00	90	91
91	50	40.3	0.0	21	0.0310	0.00	91	92
92	50	36.8	0.0	102	0.0310	0.00	92	93
93	50	28.8	0.0	179	0.0310	0.00	93	94
94	50	27.9	0.0	165	0.0310	0.00	94	95
95	50	24.3	0.0	150	0.0310	0.00	95	96
96	50	33.9	0.0	136	0.0310	0.00	96	97
97	50	18.7	0.0	134	0.0310	0.00	97	98
98	50	19.5	0.0	122	0.0310	0.00	98	99
99	50	19.1	0.0	134	0.0310	0.00	99	100
100	50	20.5	0.0	134	0.0310	0.00	100	101
101	50	23.2	0.0	136	0.0310	0.00	101	102
102	50	22.5	0.0	136	0.0310	0.00	102	103

\*\*\*\*\* CONSTANT INFLOWS/OUTFLOWS \*\*\*\*\*

0

\*\*\*\*\* VARIABLE INFLOWS/OUTFLOWS \*\*\*\*\*

1

1 64

1 0300	-9.83	1 0600	-9.83	1 0900	-9.83	1 1200	-9.94
1 1500	-9.94	1 1800	-9.83	1 2100	-9.83	1 2399	-9.71
2 0300	-9.60	2 0600	-9.60	2 0900	-9.49	2 1200	-9.37
2 1500	-9.26	2 1800	-9.15	2 2100	-9.03	2 2399	-9.03
3 0300	-8.92	3 0600	-8.81	3 0900	-8.69	3 1200	-8.58
3 1500	-8.47	3 1800	-8.35	3 2100	-8.24	3 2399	-8.16
4 0300	-8.04	4 0600	-7.93	4 0900	-7.82	4 1200	-7.82
4 1500	-7.70	4 1800	-7.62	4 2100	-7.50	4 2399	-7.39
5 0300	-7.39	5 0600	-7.39	5 0900	-7.39	5 1200	-7.31
5 1500	-7.82	5 1800	-8.81	5 2100	-9.71	5 2399	-10.2
6 0300	-11.38	6 0600	-12.89	6 0900	-14.16	6 1200	-15.35
6 1500	-16.28	6 1800	-17.11	6 2100	-17.93	6 2399	-18.49
7 0300	-18.92	7 0600	-19.34	7 0900	-19.63	7 1200	-19.63
7 1500	-19.63	7 1800	-19.63	7 2100	-19.48	7 2399	-19.20
8 0300	-18.92	8 0600	-18.49	8 0900	-18.35	8 1200	-18.18
8 1500	-18.01	8 1800	-17.16	8 2100	-16.94	8 2399	-16.77

\*\*\*\*\* DOWNSTREAM BOUNDARY DATA \*\*\*\*\*

1

3 103 64 0 0 0 0 1.0

1 0300	-1.48	1 0600	-1.48	1 0900	-1.48	1 1200	-1.48
1 1500	-1.48	1 1800	-1.48	1 2100	-1.48	1 2399	-1.48
2 0300	-1.51	2 0600	-1.51	2 0900	-1.51	2 1200	-1.51
2 1500	-1.52	2 1800	-1.52	2 2100	-1.52	2 2399	-1.52

Input File.... Continued

3 0300	-1.55	3 0600	-1.55	3 0900	-1.55	3 1200	-1.55
3 1500	-1.58	3 1800	-1.58	3 2100	-1.58	3 2399	-1.58
4 0300	-1.59	4 0600	-1.59	4 0900	-1.59	4 1200	-1.59
4 1500	-1.59	4 1800	-1.59	4 2100	-1.59	4 2399	-1.59
5 0300	-1.60	5 0600	-1.60	5 0900	-1.60	5 1200	-1.60
5 1500	-1.48	5 1800	-1.48	5 2100	-1.48	5 2399	-1.48
6 0300	-1.37	6 0600	-1.37	6 0900	-1.37	6 1200	-1.37
6 1500	-1.26	6 1800	-1.26	6 2100	-1.26	6 2399	-1.26
7 0300	-1.20	7 0600	-1.20	7 0900	-1.20	7 1200	-1.20
7 1500	-1.19	7 1800	-1.19	7 2100	-1.19	7 2399	-1.19
8 0300	-1.23	8 0600	-1.23	8 0900	-1.23	8 1200	-1.23
8 1500	-1.26	8 1800	-1.26	8 2100	-1.26	8 2399	-1.26

\*\*\*\*\* WIND DATA \*\*\*\*\*

0

\*\*\*\*\* PRECIPITATION OR EVAPORATION DATA \*\*\*\*\*

0

\*\*\*\*\* JUNCTION GEOMETRY DATA \*\*\*\*\*

0

\*\*\*\*\* CHANNEL GEOMETRY DATA \*\*\*\*\*

0

\*\*\*\*\* MAP TO WASP4 \*\*\*\*\*

0 0

## Appendix C Field Data

Day	Time	Discharge at Farm Lane Bridge	Head at Kalamazoo Bridge	Library Bridge			Kellogg Bridge		
				Head	Vel	Flow	Head	Vel	Flow
1	3:00	9.83							
	6:00	9.83							
	9:00	9.83	-1.48						
	12:00	9.94					0	0.51	10.26
	15:00	9.94							
	18:00	9.83	-1.48	0.48	0.53	9.12			
	21:00	9.83							
	0:00	9.71							
2	3:00	9.60							
	6:00	9.60							
	9:00	9.49	-1.51						
	12:00	9.37		0.47	0.53	8.89			
	15:00	9.26							
	18:00	9.15	-1.52				-0.03	0.49	9.65
	21:00	9.03							
	0:00	9.03							
3	3:00	8.92							
	6:00	8.81							
	9:00	8.69	-1.55						
	12:00	8.58		0.46	0.54	9.06			
	15:00	8.47							
	18:00	8.35	-1.58				-0.05	0.45	8.45
	21:00	8.24							
	0:00	8.16							
4	3:00	8.04							
	6:00	7.93							
	9:00	7.82	-1.59						
	12:00	7.82		0.44	0.5	8.1			
	15:00	7.70							
	18:00	7.62	-1.59				-0.07	0.41	7.55
	21:00	7.50							
	0:00	7.39							
5	3:00	7.39							
	6:00	7.39							
	9:00	7.39	-1.6						
	12:00	7.31					-0.09	0.4	7.09
	15:00	7.82							

Field Data ...continued

Day	Time	Discharge at Farm Lane Bridge	Head at Kalamazoo Bridge	Library Bridge			Kellogg Bridge		
				Head	Vel	Flow	Head	Vel	Flow
	18:00	8.81	-1.48						
	21:00	9.71							
	0:00	10.20							
6	3:00	11.38							
	6:00	12.89							
	9:00	14.16	-1.37						
	12:00	15.35		0.65	0.61	15.4			
	15:00	16.28							
	18:00	17.11	-1.26				0.05	0.69	13.69
	21:00	17.93							
	0:00	18.49							
7	3:00	18.92							
	6:00	19.34							
	9:00	19.48	-1.2	0.89	0.61	19.8			
	12:00	19.63					0.56	0.62	21.96
	15:00	19.63							
	18:00	19.63	-1.19						
	21:00	19.48							
	0:00	19.20							
8	3:00	18.92							
	6:00	18.49							
	9:00	18.07	-1.23	0.82	0.62	18.17			
	12:00	17.64					0.51	0.57	18.47
	15:00	17.25							
	18:00	16.82	-1.26						
	21:00	16.43							
	0:00	16.00							

Note: Filed data collected was from 04 April 2002 to 11 April, 2002.

## Appendix D Time-Concentration Data-Dye Release 1

Farm Lane Bridge		Kellogg Foot Bridge		Kalamazoo Bridge	
Time since Injection	Dye Conc.	Time since Injection	Dye Conc.	Time since Injection	Dye Conc.
(mins)	(ug/L)	(mins)	(ug/L)	(mins)	(ug/L)
45.13	0.04	97.03	0.00	146.88	0.03
46.15	0.50	99.00	1.39	148.92	0.96
47.15	0.74	101.00	4.65	150.95	2.82
48.15	0.97	103.00	6.51	153.00	4.68
49.15	0.97	105.02	9.77	155.03	5.61
50.13	2.83	107.08	12.56	157.12	7.47
51.15	7.94	109.00	13.95	159.15	8.40
52.15	15.15	111.03	16.28	161.15	10.26
53.15	25.15	113.07	17.90	163.18	10.73
54.13	18.64	115.02	17.67	165.25	12.12
55.17	35.38	117.00	16.74	167.28	12.82
56.15	34.45	119.00	16.74	169.33	13.05
57.13	36.31	121.00	16.74	171.73	13.52
58.15	37.24	123.00	14.88	173.78	13.05
59.15	40.96	125.02	20.46	175.72	15.38
60.15	27.48	127.03	13.49	177.77	12.35
61.13	34.45	129.02	12.09	180.02	11.19
62.15	32.83	131.02	11.16	182.08	10.73
63.15	28.87	133.00	14.88	184.05	10.73
64.13	25.15	135.02	9.30	186.07	8.40
65.15	23.29	137.00	8.37	188.33	8.17
66.17	20.50	139.00	7.44	190.40	7.00
67.15	20.73	141.00	6.51	194.00	6.02
68.15	17.71	143.02	5.58	198.00	4.97
69.13	15.85	145.00	4.65	202.00	4.10
70.15	14.46	147.00	4.18	206.00	3.38
71.15	14.46	149.00	3.72	210.00	2.79
72.15	11.90	151.02	2.79	214.00	2.30
73.15	11.20	153.03	1.86	218.00	1.90
74.15	12.13	155.00	1.86	222.00	1.57
75.15	9.34	157.00	1.39	226.00	1.30
76.13	9.34	159.00	0.93	230.00	1.07
77.15	7.71	161.00	0.93	234.00	0.88
78.15	6.55	163.00	0.93	238.00	0.73
79.15	6.08	165.00	0.00	242.00	0.60

Time-Concentration Data - Dye Release 1.... Continued



Farm Lane Bridge		Kellogg Foot Bridge		Kalamazoo Bridge	
Time since injection	Dye Conc.	Time since injection	Time since injection	Dye Conc.	Time since injection
(mins)	(ug/L)	(mins)	(mins)	(ug/L)	(mins)
80.17	4.69			246.00	0.50
81.15	3.76			250.00	0.41
82.15	3.76			254.00	0.34
83.15	2.83			258.00	0.28
84.15	5.62			262.00	0.23
85.15	1.90			266.00	0.19
86.17	1.90			270.00	0.16
				274.00	0.13

Note: - 2.65 Litres of Fluorescein Dye Released at 10:00 am on May 17, 2002.

## Appendix E Time-Concentration Data-Dye Release 2

Farm Lane Bridge		Kellogg Foot Bridge		Kalamazoo Bridge	
Time since injection	Dye Conc. (ug/L)	Time since injection	Dye Conc. (ug/L)	Time since injection	Dye Conc. (ug/L)
<i>(mins)</i>	<i>(ug/L)</i>	<i>(mins)</i>	<i>(ug/L)</i>	<i>(mins)</i>	<i>(ug/L)</i>
53.92	1.11	109.28	2.98	154.00	0.49
54.92	1.34	111.33	15.22	157.00	1.42
55.90	4.57	112.37	9.67	160.00	3.26
56.90	12.42	113.40	13.37	163.00	5.57
57.92	19.35	114.43	17.52	166.00	8.34
58.95	38.97	115.45	19.60	169.00	12.04
59.92	60.90	116.45	27.22	172.00	16.19
60.92	71.98	117.47	26.76	174.00	19.42
61.92	86.76	118.55	29.07	176.00	20.81
62.92	85.37	119.58	32.76	178.00	22.66
63.92	83.99	120.60	33.22	180.00	24.04
64.92	82.60	121.60	33.68	182.00	24.96
65.92	71.52	122.60	34.61	184.00	25.43
66.92	70.14	123.62	35.07	186.00	24.96
67.92	64.60	124.67	35.99	188.00	25.89
68.92	59.06	125.68	34.15	190.00	26.35
69.92	50.28	126.70	34.15	192.00	26.81
70.92	44.28	127.72	33.68	194.00	25.43
71.92	38.74	128.78	33.22	196.00	24.04
72.92	36.89	129.80	33.22	198.00	22.42
73.92	32.97	130.80	32.99	200.00	21.27
74.92	30.89	131.88	31.84	202.00	21.27
75.92	28.58	132.95	30.45	204.00	20.35
76.92	29.97	133.97	29.53	206.08	18.50
77.92	29.04	134.98	29.07	208.00	16.65
78.95	20.27	136.12	26.99	210.00	15.73
79.93	21.66	137.13	26.30	212.00	15.73
80.93	20.27	138.13	23.99	214.00	14.81
81.92	18.42	139.15	24.45	216.00	16.65
82.92	19.35	140.17	23.53	218.00	13.19
83.92	20.27	141.20	22.37	220.00	12.04
84.92	19.35	142.27	22.60	222.00	10.65

Time-Concentration Data - Dye Release 2...continued

Farm Lane Bridge		Kellogg Foot Bridge		Kalamazoo Bridge	
Time since Injection	Dye Conc. (ug/L)	Time since Injection	Time since Injection	Dye Conc. (ug/L)	Time since Injection
(mins)	(ug/L)	(mins)	(mins)	(ug/L)	(mins)
85.92	12.88	143.30	21.22	224.00	10.19
86.92	11.50	144.32	20.29	226.00	9.27
88.25	9.65	145.33	19.37	228.00	8.57
89.25	9.19	146.37	19.14	230.00	7.88
90.25	9.19	147.40	17.52	232.00	7.88
91.25	8.27	148.47	17.06	234.00	7.88
93.25	12.42	149.55	16.14	236.00	6.96
95.25	11.50	150.57	15.22	238.00	6.03
96.27	5.96	151.60	14.75	240.00	6.03
97.28	3.65	153.70	13.37	242.17	8.34
		155.70	11.98	244.00	5.57
		158.02	10.60	246.00	6.50
		160.03	9.21	248.00	4.65
		162.03	8.06	251.00	3.73
		164.10	7.37	254.00	4.65
		166.10	6.90	257.00	4.19
		168.12	6.90	260.00	2.80
		170.10	5.06	263.00	2.34
		172.13	3.90	266.00	2.34
		174.15	3.67	269.00	2.34
				272.00	1.88
				275.00	1.42
				278.00	0.95
				281.00	1.88
				284.00	0.95
				287.00	0.95
				290.00	0.95
				293.00	1.42
				296.00	0.95
				298.00	1.42
				301.10	0.95
				304.28	0.95
				307.00	1.42

Note: - 5.0 Litres of Fluorescein Dye Released at 10:00 am on May 31, 2002.

## Appendix F Time-Concentration Data-Dye Release 3

Farm Lane Bridge		Kellogg Foot Bridge		Kalamazoo Bridge	
Time since Injection	Dye Conc.	Time since Injection	Dye Conc.	Time since Injection	Dye Conc.
(mins)	(ug/L)	(mins)	(ug/L)	(mins)	(ug/L)
41.37	0.00	91.02	1.35	118.00	0.00
42.37	0.44	92.02	3.54	118.00	0.84
43.37	0.00	93.02	4.41	122.00	0.84
45.33	2.62	94.02	7.48	125.00	0.40
47.33	4.37	95.02	10.54	128.00	0.40
48.33	19.25	96.03	14.48	132.00	0.84
49.33	47.69	97.05	17.98	135.00	1.27
50.33	54.69	98.02	20.60	138.00	3.46
51.33	67.82	99.03	25.85	141.00	6.53
52.33	79.63	100.12	27.60	144.00	10.90
53.33	74.38	101.03	29.57	147.00	15.71
54.33	78.32	102.17	31.98	149.00	17.90
55.35	73.07	103.03	32.85	151.00	21.40
56.33	59.94	104.03	33.29	153.00	23.59
57.33	49.44	105.00	35.48	155.00	24.90
58.33	56.88	106.07	36.79	157.00	27.31
59.33	55.56	107.00	36.79	159.00	27.53
60.33	30.20	108.02	36.79	161.00	27.53
61.33	35.88	109.03	36.79	163.00	28.40
62.33	37.19	110.02	36.35	165.00	27.96
63.33	37.19	111.10	36.79	167.00	28.40
64.33	30.63	112.02	35.91	169.00	27.53
65.35	32.70	113.00	34.16	171.00	26.21
66.33	22.75	114.03	34.16	173.00	25.78
67.33	19.69	115.00	31.98	175.00	24.03
68.33	20.56	116.20	31.54	177.00	23.15
69.33	20.13	117.00	30.23	179.00	21.40
70.33	35.20	118.00	30.66	181.00	19.65
71.33	18.81	119.00	29.35	183.00	19.21
72.33	14.00	120.50	27.60	185.00	17.46
73.33	11.38	121.25	27.82	187.00	15.49
74.33	12.69	122.00	25.85	189.00	13.09
75.33	37.70	123.00	24.98	191.00	13.53
76.33	9.63	124.00	23.66	193.00	12.65
77.35	9.19	125.00	22.79	195.00	10.90
78.33	7.44	126.00	21.91	197.00	11.12

Time - Concentration Data - Dye Release 3...continued

Farm Lane Bridge		Kellogg Foot Bridge		Kalamazoo Bridge	
Time since Injection	Dye Conc.	Time since Injection	Time since Injection	Dye Conc.	Time since Injection
(mins)	(ug/L)	(mins)	(mins)	(ug/L)	(mins)
79.33	6.56	127.00	21.04	199.00	9.59
80.33	40.20	129.33	17.98	201.00	8.28
81.37	7.00	130.00	17.10	203.00	7.84
82.35	7.00	131.00	17.10	205.00	7.40
83.33	5.25	132.00	14.48	207.00	6.96
85.33	42.70	133.00	15.35	209.00	5.65
86.33	2.62	135.35	13.60	211.00	6.09
87.35	2.62	137.33	12.29	213.00	5.21
88.33	2.19	139.00	10.10	215.00	4.77
89.33	2.19	141.00	9.66	217.00	4.34
90.35	45.20	143.00	7.48	219.00	3.90
91.35	1.75	145.00	6.60	221.00	3.90
92.33	1.75	147.00	5.73	223.00	3.02
94.33	0.87	149.00	5.73	225.00	3.02
95.35	47.70	151.00	4.85	227.00	3.02
96.33	1.31	153.00	3.54	229.00	2.59
97.33	0.87	155.00	3.10	232.00	2.59
98.33	0.44	157.00	2.66	235.00	0.84
99.33	0.00	159.00	2.22	238.00	1.71
		161.00	2.22	241.00	2.37
		163.00	1.79	244.00	1.27
		165.00	1.35	247.00	1.27
		167.00	0.91	250.00	1.27
		169.00	0.91	253.00	0.84
		171.00	0.91	256.00	1.06
		173.00	0.47	259.00	0.84
		175.00	1.13	262.00	0.84
		177.00	0.04	265.00	0.40
		179.00	0.04	268.00	0.40
		181.00	0.04	271.00	0.40
				274.00	1.27
				277.00	1.27
				280.00	1.27
				283.00	0.84
				286.00	0.84

Note: - 6.0 Litres of Fluorescein Dye Released at 10:00 am on June 06, 2002

## Appendix G Time-Concentration Data-Dye Release 4

Bogue Bridge (Left)		Bogue Bridge (Centre)		Bogue Bridge (Right)	
Time since Injection	Dye Conc	Time since Injection	Dye Conc	Time since Injection	Dye Conc
(mins)	(ug/L)	(mins)	(ug/L)	(mins)	(ug/L)
61.00	0.00	127.13	0.00	101.88	0.00
66.00	0.03	129.13	0.87	133.50	3.07
72.00	0.03	131.22	11.78	135.40	1.32
129.00	3.09	133.13	24.44	137.40	8.31
132.00	0.90	135.12	21.82	139.30	23.59
134.00	5.71	136.88	42.78	141.27	41.27
136.00	7.89	138.90	53.69	143.30	23.59
138.00	7.45	140.83	62.43	145.30	28.39
140.00	15.75	142.88	65.48	147.27	38.87
142.00	55.04	144.95	66.35	149.17	51.97
144.00	25.79	146.95	68.10	151.27	59.39
146.00	29.28	148.93	68.97	153.27	47.60
148.00	27.97	150.97	71.59	155.28	65.06
150.00	22.73	152.97	71.59	157.27	52.84
152.00	40.63	154.95	48.02	159.28	63.32
154.00	41.07	156.93	63.74	161.33	55.68
156.00	51.98	158.93	47.15	163.27	57.20
158.00	38.89	160.92	43.87	165.20	55.46
160.00	34.52	162.97	42.34	167.22	49.35
162.00	34.96	164.93	42.78	169.23	47.60
164.00	35.83	167.10	38.41	171.33	43.67
166.00	39.32	169.05	30.56	173.00	42.36
168.00	34.08	171.05	27.06	175.00	37.99
170.00	34.08	173.07	27.94	177.00	38.43
172.00	35.83	175.07	23.57	179.00	41.05
174.00	34.08	177.07	29.68	181.00	40.18
176.00	31.46	179.07	22.26	183.00	31.88
178.00	28.41	181.05	18.11	185.00	36.69
180.00	29.28	183.12	12.66	187.00	25.77
182.00	27.97	185.12	13.97	189.00	26.21
184.00	28.41	187.12	13.53	191.00	23.59
186.00	25.79	189.08	16.59	193.00	24.90
188.00	26.44	191.10	16.80	195.00	27.08
191.00	20.55	193.08	13.97	197.00	18.79
193.00	23.61	195.07	9.60	199.00	19.66
195.00	18.37	197.05	10.47	201.00	26.64

Concentration Data - Dye Release 4...continued

Bogue Bridge (Left)		Bogue Bridge (Centre)		Bogue Bridge (Right)	
Time since Injection	Dye Conc	Time since Injection	Time since Injection	Dye Conc	Time since Injection
(mins)	(ug/L)	(mins)	(mins)	(ug/L)	(mins)
197.00	21.42	199.08	9.60	203.00	17.04
199.00	20.11	201.10	8.73	206.00	16.17
201.00	22.30	203.08	11.35	208.00	17.04
203.00	21.86	205.07	9.60	211.00	13.98
205.00	20.11	207.03	8.73	213.00	11.80
207.00	18.37	209.05	7.42		
209.00	18.58	211.10	8.29		
211.00	18.37	213.05	4.36		
213.00	16.18				

Note: - 2.0 Litres of Fluorescein Dye Released at 10:00 am on June 21, 2002

## Appendix H Time-Concentration Data-Dye Release 5

Farm Lane Bridge		Kalamazoo Bridge	
Time since Injection	Dye Conc.	Time since Injection	Dye Conc.
(mins)	(ug/L)	(mins)	(ug/L)
271.00	0.00	585.00	0.00
273.00	0.24	588.00	1.15
275.00	1.23	591.00	1.54
277.00	0.44	594.00	0.00
279.00	1.23	597.00	0.16
281.00	3.99	600.00	0.36
283.00	1.43	603.00	0.36
285.00	2.02	606.00	0.00
287.00	3.20	609.00	0.36
289.00	2.81	612.00	0.16
291.00	2.02	615.00	0.36
293.00	3.01	618.00	0.36
295.00	3.60	621.00	0.00
297.00	4.78	624.00	0.00
299.00	4.78	627.00	0.95
301.00	7.15	630.00	1.15
303.00	6.76	633.00	1.15
305.00	8.34	636.00	1.54
307.00	7.94	639.00	1.15
309.00	15.84	642.00	0.95
312.00	11.10	645.00	1.15
315.00	7.55	648.00	1.15
321.00	11.89	651.00	1.54
324.00	13.47	654.00	1.54
327.00	15.05	657.00	1.54
330.00	8.73	660.00	3.12
333.00	8.93	663.00	1.94
336.00	10.31	666.00	2.33
339.00	11.50	669.00	2.73
342.00	7.94	672.00	2.33
345.00	8.34	675.00	2.73
350.00	7.15	678.00	2.73
353.00	8.73	681.00	3.12
356.00	9.52	684.00	3.52
359.00	7.15	687.00	3.12
362.00	7.94	690.00	3.52
365.00	8.53	693.00	3.12
368.00	7.55	696.00	3.12
371.00	4.78	699.00	3.91
374.00	6.36	702.00	3.12
377.00	5.57	705.00	3.91

Concentration Data - Dye Release 5...continued



Farm Lane Bridge		Kalamazoo Bridge	
Time since injection	Dye Conc.	Time since injection	Dye Conc.
(mins)	(ug/L)	(mins)	(ug/L)
380.00	4.59	708.00	3.91
383.00	5.18	711.00	3.91
386.00	3.99	714.00	3.91
389.00	5.57	717.00	3.32
392.00	2.41	720.00	3.91
395.00	2.81	723.00	3.91
		726.00	3.91
		729.00	4.31
		732.00	3.72
		735.00	3.91
		738.00	3.91
		741.00	3.91
		744.00	3.91
		747.00	3.91
		750.00	3.91
		753.00	4.31
		756.00	4.31
		759.00	3.91
		762.00	3.91
		765.00	3.91
		768.00	4.70
		771.00	4.31
		774.00	4.31
		777.00	3.91
		780.00	4.31

Note: - 1.0 Litres of Fluorescein Dye Released at 10:00 am on June 25, 2002

## 8. BIBLIOGRAPHY

- Ambrose, R. B. (1988). A Hydrodynamic and Water Quality Model. Model Theory, User's Manual and Programmer's Guide, U.S environment Protection Agency, Athens, Georgia.
- Ambrose, R. B. (1993). The Dynamic Estuary Model, Hydrodynamics Program, DYNHYD5, Model Documentation and User's Manual, ASCI Corporation, Athens, Georgia.
- Brown, L. C and T.O. Barnwell Jr. (1987). The Enhanced Stream Water Quality Models QUAL2E and QUAL2E-UNCAS: Documentation and User's Manual. Environmental Research Laboratory, U.S Environment Protection Agency, Athens, Georgia.
- Chow, V. T. (1959). Open Channel Hydraulics. New York, McGraw-Hill.
- Coon, W. F. (1998). Estimation of Roughness Coefficients for Natural Stream Channels with Vegetated Banks, U.S Geological Survey, U.S Department of Interior.
- Davis, P. M., T. C. Atkinson, et al. (2000). "Longitudinal Dispersion in Natural Channels. The Roles of Shear Flow Dispersion and Dead Zones in the River Severn, U.K." Hydrology and Earth System sciences 4(3): 355-371.
- Davood, H. (1960). Hydrologic Studies On The Cedar River Basin. Department Of Agricultural engineering, Michigan State University, East Lansing.
- Deng, Z. Q, Singh, V.P, et al (2001). "Longitudinal Dispersion Coefficient in Straight Rivers." Journal of Hydraulic Engineering 127(11): 919-927
- Fischer, H. B. (1981). Transport Models for Inland and Coastal waters. New York, Academic Press.
- Jennings, M.E., Shearman, J.O, Bauer, D.P (1976). Selection Of Stream flow and Reservoir Release Models for River Water Quality Assessment, U.S Geological Survey.
- Kasnavia, Tomez., and Sabatini, David. A. (1999). "Fluorescent Dye and Media Properties Affecting Sorption and Tracer Selection." Ground Water 37(3): 376-381
- Kashefipour, S. M. and R. A. Falconer (2002). "Longitudinal Dispersion Coefficients in Natural Channels." Water Research 36(6): 1596-1608.

- Koussis, A. D. and J. R. Mirasol (1998). "Hydraulic Estimation of Dispersion Coefficients for Streams." Journal of Hydraulic Engineering **124**(3): 317-320.
- Schaffranek, R. A. B. and D. E. Goldberg (1981). A Model For Simulation of Flow in Singular and Interconnected Channels. U.S Geological Survey, U.S Department of Interior.
- Seo, W. and T. S. Cheong (1998). "Predicting Longitudinal Dispersion Coefficient in Natural Streams." Journal of Hydraulics Engineering **124**(1): 25-32.
- Seo, W. and T. S. Cheong (2001). "Moment-Based Calculation of Parameters for The Storage Zone Model for River Dispersion." Journal of Hydraulics Engineering **127**(6): 453-465.
- Smart, P. L. and I. M. S. Laidlaw (1977). "An Evaluation of Some Fluorescent Dyes for Water Tracing." Water Resources Research **13**(1): 15-33.
- Swamee, P. K., S. K. Pathak, et al. (2000). "Empirical Relations for Longitudinal Dispersion in Streams." Journal of Environmental Engineering **126**(11): 1056-1062.
- Thoman, R. V. (1982). "Verification of water Quality Models." Journal of Environmental Engineering **108**: 923-940.
- Thomann, R. V. (1982). "Verification of water Quality Models." Journal of Environmental Engineering **108**(5): 923-940.
- Wu, Y. t. (1995). Calibration And Validation of The DYNHYD5, Hydrodynamic Model For The Delaware River Estuary. West Trenton, New Jersey. Estuary Toxics Management Program, Delaware River Basin Commission.

MICHIGAN STATE UNIVERSITY LIBRARIES



3 1293 02427 1177